P 2.11X

NATIONAL AERONAUTICS AND SPACE ADMINISTRATION

Technical Memorandum 33-668

Solar Array Study for Solar Electric Propulsion Spacecraft for the Encke Rendezvous Mission

E. A. Sequeira

R. E. Patterson

JET PROPULSION LABORATORY

CALIFORNIA INSTITUTE OF TECHNOLOGY

PASADENA, CALIFORNIA

February 1, 1974

Prepared Under Contract No. NAS 7-100
National Aeronautics and Space Administration

PREFACE

The work described in this report was performed by the Guidance and Control Division of the Jet Propulsion Laboratory.

ACKNOWLEDGEMENTS

The cooperation and contributions of the people who supported the SEPSIT Solar Array study are greatly appreciated. J.C. Arnett, E.R. Bunker, Jr., E.N. Costogue, R.G. Ross, B.C. Fletcher, E.A. Sequeira, and R.E. Patterson were primarily responsible for the technical contents of the study. J.V. Goldsmith, B. Anspaugh, and R. Yasui provided data and valuable suggestions.

CONTENTS

CONTENTS (contd)

TABLES

TABLES (contd)

FIGURES

FIGURES (contd)

ABSTRACT

This document describes the work performed during 1973 on the design, analysis and performance of a 20kW Rollup Solar Array capable of meeting the design requirements of a solar electric spacecraft for the 1980 Encke rendezvous mission. To meet the high power requirements of the proposed electric propulsion mission, solar arrays on the order of 186.6 m^2 have been defined. Because of the large weights involved with arrays of this size, consideration of array configurations is limited to lightweight, large area concepts with maximum power-to-weight ratios.

Items covered in this document include solar array requirements and constraints, array concept selection and rationale, structural and electrical design considerations, and reliability considerations. The study was concluded by identifying the areas which require further study.

I. INTRODUCTION

This document describes the work performed during 1973 on the Solar Electric Propulsion System Integration Technology (SEPSIT) Solar Array Study. The purpose of the study was to functionally describe a 20 kW Rollup Solar Array capable of meeting design requirements of a solar electric spacecraft for a 1980 Encke Rendezvous Mission. Section II describes the Encke Rendezvous Mission and identifies the solar array requirements and constraints. The solar array concept selection is described in Section III. The solar options are discussed as well as the selection rationale for the General Electric Array Concept. Section IV is devoted to describing the General Electric Solar Array Concept. Items covered in this section include system design, array blankets, solar panel actuator, slip ring assembly, structural components and mass properties summary. In addition, prototype tests and results are described. Unmodified, the General Electric solar array concept is not capable of interfacing with the solar electric spacecraft and meeting all of the imposed requirements. Thus, significant modifications were made to the GE concept. Section V discusses the application of the GE solar array concept to the SEPSIT requirements. Structural design considerations are discussed including a discussion of prototype scale-up considerations. Electrical design considerations are discussed which include cell characteristics, voltage range selection, radiation effects, cabling losses, and uncertainty. The actual electrical design configuration is discussed in detail together with electrical performance predictions at 200-day intervals throughout the Encke rendezvous mission. Additional studies presented in Section V include cabling, and interfaces. Section VI discusses reliability considerations. Section VII completes the study with a discussion of areas requiring further work.

II. SEPSIT MISSION

The application of solar electric propulsion (SEP) technology for exploring space beyond the reach of ballistic missions has been investigated by JPL for many years. Recently, the application of this technology has concentrated on an Encke Rendezvous mission with a 1978 scheduled launch date. A major consideration in power subsystem design studies for a solar electric mission in this time frame is that only minor modifications in existing technology could be considered. Major technology improvements would be outside the scope of considerations required to realistically define the spacecraft.

The Encke rendezvous mission requires that the electric propulsion subsystem provide thrust during the entire mission trajectory which extends from Earth at 1.0 AU to 3.3 AU and returns to 1.0 AU for rendezvous with the comet.

The solar array design selected to meet the above mission has evolved from the rollup solar array JPL development program initiated in 1967. The rationale for the selection of the JPL/GE rollup solar array over other lightweight solar array concepts is discussed in Section III of this document. The requirements and constraints imposed on the solar array design are outlined below:

A. Solar Array Requirements and Constraints

1. Performance

(1) Power

The solar array shall be designed to supply power in accordance with the power utilization summary shown in Table 1.

(2) Voltage

The array voltage shall be in the range of 200 to 400 volts throughout the mission during steady state mode.

(3) Telemetry

The solar array shall provide telemetry output sufficient to denote its status.

Table 1. Power Utilization Summary

Flight Phases	① Liftoff	② Sun Acquis. & Batt. Chg.	③ (6 Thrust) and Cru. Sci.	④ / ⑫ (5 Thrust) and Cru. Sci.	⑤ / ⑪ (4 Thrust) and Cru. Sci.	⑥ / ⑩ (3 Thrust) and Cru. Sci.	⑦ / ⑨ (2 Thrust) and Cru. Sci.	⑧ (1 Thrust) and Cru. Sci.	⑬ (6 Thrust) and Eng. Sci.
Power source	Battery	S/A	S/A	S/A	S/A	S/A	S/A	S/A	S/A
Time in days	1 Hr	2	36	24/16	28/14	41/32	118/96	540	
Spacecraft, W	393	545	360	374	360	360	360	360/292	530
SEP modules, W	267	420	163	143	139	118	115	99	163
Thruster pwr cond, W	0	0	15,500	14,400	11,520	8,640	5,760	2880/1440	15,350
Dist losses, W	0	20	200	160	120	100	80	60/40	200
SEP veh totals, W	412	965	16,223	15,077	12,139	9,218	6,315	3399/1871	16,243
1% power marg, W	-	96	162	150	121	92	63	34/19	162
S/A design pwr, W	-	1,061	16,385	15,227	12,260	9,310	6,378	3433/1890	16,405

2. Structural

(1) Dimensions

The solar array volume and shape in stowed configuration, including the release and deployment mechanisms, shall satisfy the following requirements:

(a) Launch vehicle shroud volume restrictions

(b) Spacecraft structural interface requirements

(c) Solar Array deployment complexity (reliability)

(2) Weight

The solar array weight shall be such that the specific power to weight ratio exceeds 66 watts per kilogram at a solar intensity of 140 mW/cm^2 (1 AU) and a temperature of 52.0°C.

(3) Structural Rigidity-stowed Configuration

The solar array shall be designed to pass the launch vibration and shock levels not determined at the present time.

3. Environmental

(1) Vacuum

The solar array shall be designed to operate mechanically in a vacuum of 10^{-6} torr or less.

(2) Thermal

The solar array shall be designed to operate mechanically at temperatures in the range of 52°C to -100°C.

(3) Radiation

Solar array proton degradation design margin shall be in accordance with the radiation environment specified in "Environmental Design Criteria for SEPSIT."

(4) General

The solar array shall be designed to operate in a controllable manner while being exposed to the various environments specified in "Environmental Design Criteria for SEPSIT."

4. Component and Material Selection. Wherever possible the solar array shall be designed in accordance with 66 watts/Kg rollup array technology. Specific constraints include the use of:

(1) 0.020 cm, 2 cm × 2 cm, N/P silicon solderless solar cells.

(2) 0.08 cm microsheet coverglass.

(3) Silver expanded metal interconnection for solar cells.

(4) 0.005 cm Kapton substrate sheet.

5. Reliability. The solar array design shall incorporate design practices that maximize the probability that the solar array will operate successfully in both mechanical and electrical modes.

III. SOLAR ARRAY CONCEPT SELECTION AND RATIONALE

To meet the high power requirements of the proposed electric propulsion mission, very large solar array areas, on the order of 92.9 to 185.8 m^2 (1000 to 2000 ft^2), have been defined. Because of the large weights involved with arrays of this size, array configurations for the Encke rendezvous spacecraft are limited to lightweight large area concepts with maximum power-to-weight ratios. In addition, the arrays must be compatible with spacecraft simplicity and array gimbaling requirements.

By arbitrarily limiting attention to concepts which promise power-to-weight ratios in excess of 66 watts per kilogram, and considering only array configurations which have previously been developed to various stages of readiness, the list of candidate arrays is reduced to the following:

(1) The GE rollup array.

(2) The Fairchild Hiller rollup array.

(3) The Ryan rollup array.

(4) The Hughes rollup array.

(5) The TRW flat pack array.

(6) The Royal Aircraft Establishment flat pack array.

(7) The Lockheed flat pack array.

(8) The Messerschmidt-Bolkow-Blohm flat pack array.

First, the GE rollup array has the following advantages:

(1) Extensive test experience.

(2) Center support mounting which allows easy array gimbaling.

(3) Structural simplicity which increases reliability and allows easy extrapolation to the much larger SEPSIT array.

(4) Partial deployment capability with full structural stiffness in the partially deployed state.

(5) Retraction capability.

In contrast, the Fairchild Hiller and Ryan rollup arrays are essentially similar to the GE array, but are more complex, have much less test experience, and are end mounted which complicates gimbaling. Though the Hughes array has extensive test experience, it simultaneously deploys two arrays in opposite directions from an end supported drum. This two array configuration is not compatible with the array orientation of the SEPSIT spacecraft.

As a class, the early flat pack arrays are less desirable because they exhibit very low structural stiffness in the partially deployed state and generally do not allow retraction. However, more recent flat packs, in particular the TRW concept and a concept currently being developed by Lockheed for the Manned Space Station, do allow retraction. These latter two concepts are single boom arrays essentially similar to the GE rollup array except that the cell blanket is Z-folded in a container instead of being rolled on a drum. Though they tend to be somewhat more compact than the GE array they do not allow partial deployment and have little if any stiffness during the deployment or retraction. The effect of this lack of stiffness on spacecraft attitude control during deployment and retraction needs to be analyzed. Generally these flat pack arrays suffer from lack of test experience.

On the advantage side, the flat pack cell blankets lend themselves to modular construction and do not require slip ring or other power transfer devices. After deployment, the arrays are center supported like the GE rollup and thus also allow easy gimbaling.

In summary, the GE rollup array is superior to other rollup arrays for SEPSIT application. Its advantage over recent flat pack concepts, in particular the TRW array, is less clear cut and is based primarily on the lack of test experience with these arrays. Because the flat packs have certain design advantages (modular blanket construction, and absence of slip rings for power transfer) their development should be watched closely. However, because they are currently in a very preliminary design stage, the GE array was adopted as the baseline array in the SEPSIT study.

IV. GE SOLAR ARRAY CONCEPT DESCRIPTION

A. General Description

An engineering test model was designed, fabricated and tested by the General Electric Company under contract to JPL. The array provides 23.2 m^2 of deployed solar cell module area and was fabricated to represent a flight-type design (Fig. 1), except for a limited solar cell coverage; 4000 solar cells were bonded to the substrates, with the remaining area occupied by glass platelets to simulate the solar cell mass and bending stiffness. The locations of the various components on the engineering test model are shown in Fig. 2.

The array power-to-weight ratio is 66 W/kg. This ratio is based on the ability of the array to generate 2500 Watts of power at 55°C under air mass zero illumination at one (1.0) AU. Cell efficiency is specified by area performance of 107.6 W/m^2 (10 W/ft^2) of gross module area. The cell selected was 0.020 cm thick, 2 cm by 2 cm, with 3.8 cm^2 of active area per cell. The calculated array power for the cell under 1 AU conditions is 2523 Watts at 102 Vdc.

The major components of the solar array system are described below:

1. Solar array substrate. The solar cells mounted on two flexible substrates of 0.005-cm Kapton H film fabricated from copper-clad Schjel-Clad L-7510 etched to form a conductor electrical bus strip system. The bus in turn connects to the feed-through section of the drum and the slip rings. The exposed copper bus strips on the rear side of the substrate are covered with Kapton silicon pressure-sensitive tape. Foamed RTV 560 cushioning buttons are deposited on the rear side of the substrate at the corners of each solar cell. These buttons provide the required interlayer, cushioning the stowed configuration.

2. Solar panel actuator. The solar panel actuator is a Bi-stem deployable boom unit designed and developed by Spar Aerospace Products, Ltd. The boom elements, the components which provide the actuation force for deployment and form the primary structure in the deployed configuration, have a nominal outside diameter of 3.4 cm (1.34 inches). The boom material is 0.018 cm (0.007 inches) thick and is prestressed to form an overlapped tube in the deployed position. The boom is silver plated on its outside surfaces to

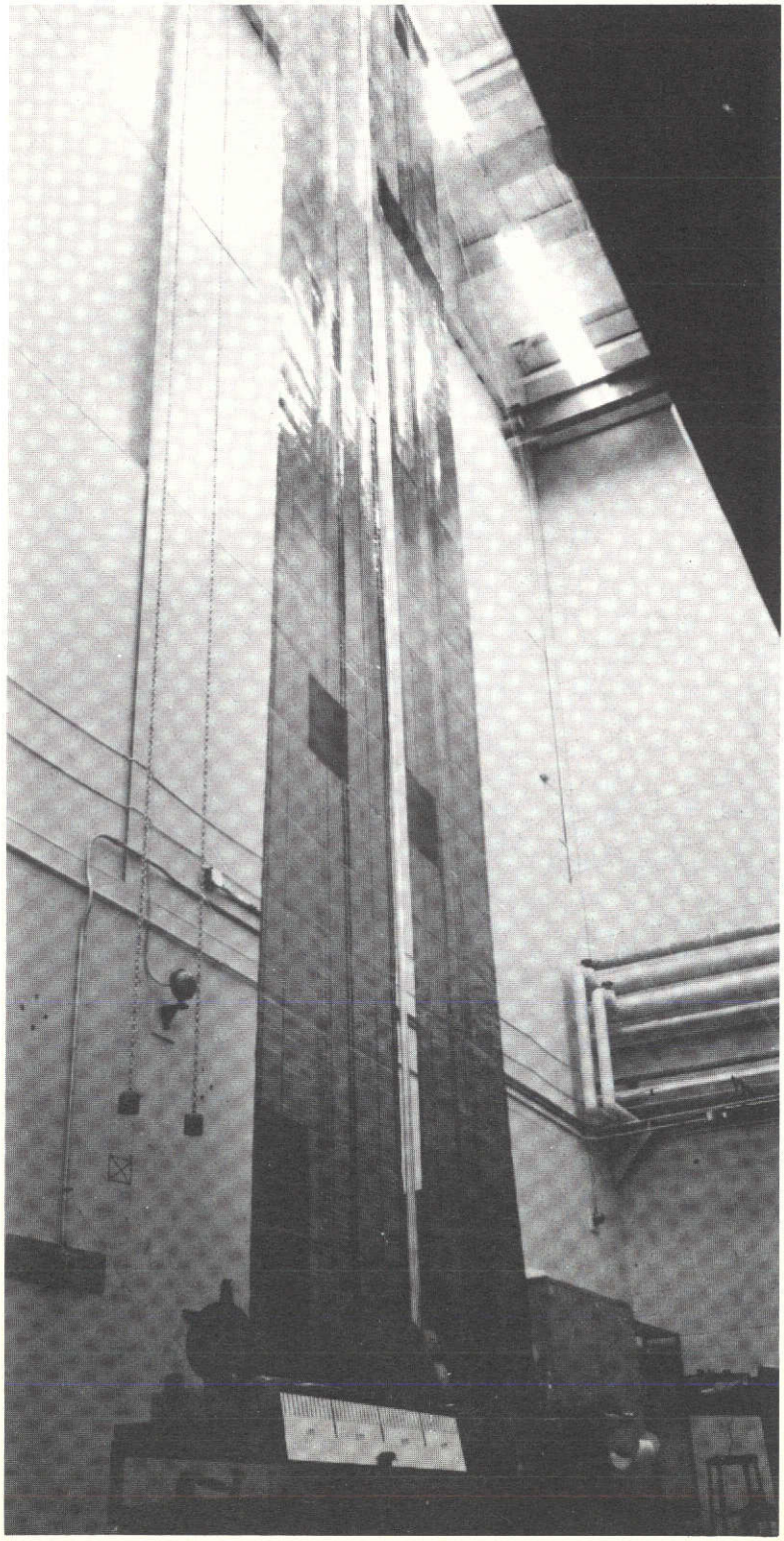

Fig. 1. Fully Deployed Solar Array

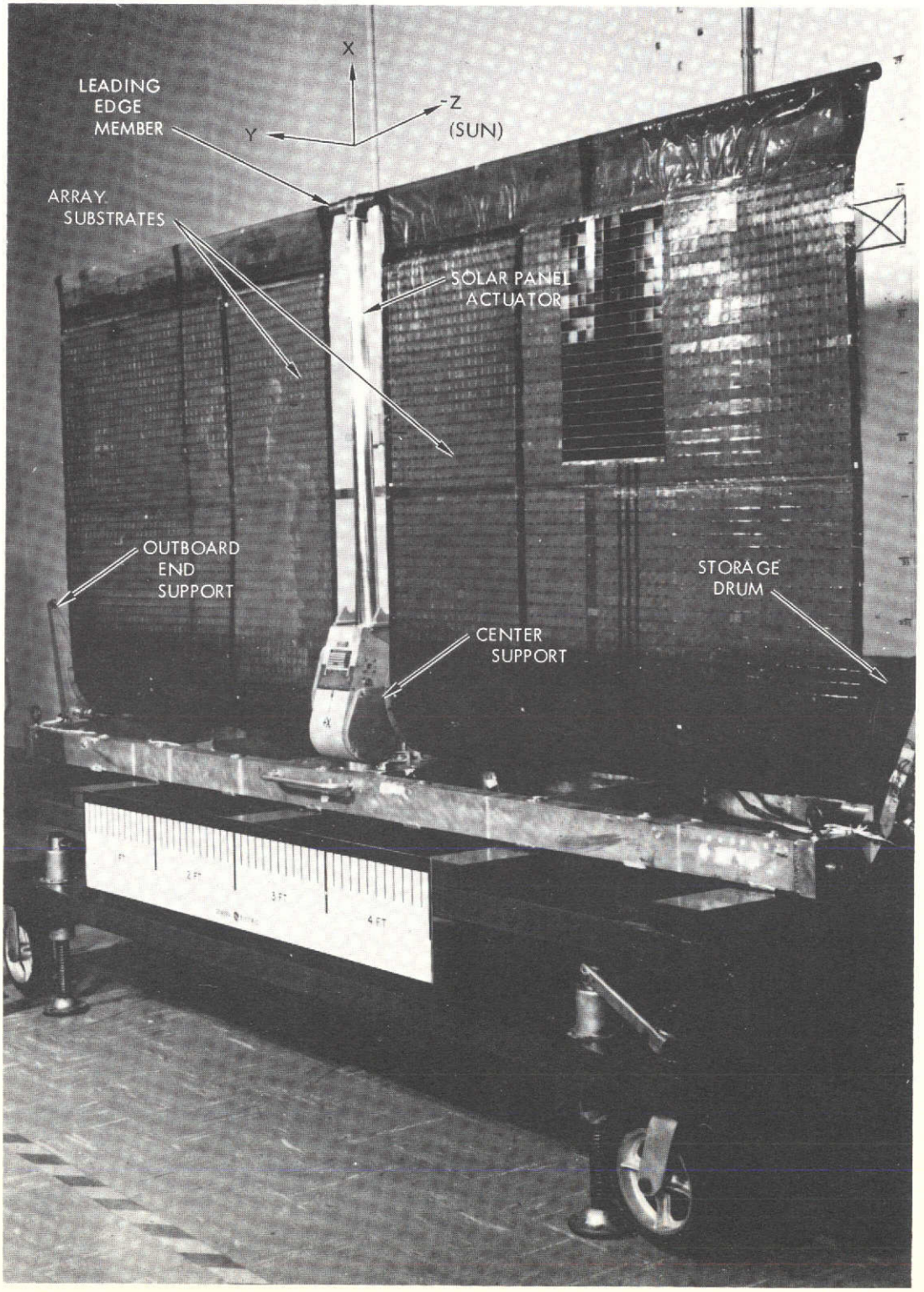

Fig. 2. Solar Array Structural Components

reduce the temperature gradients in the boom when one side is exposed to solar radiation and the other side is in shadow.

3. Storage drums. The two storage drums in the system form the backbone of the stowed configuration. The drums rotate approximately 15 turn to deploy or retract the array. Each drum includes a shell, outboard end cap, inboard end cap, and edge guides. The drum shells are 1.196 m (47.10 inches) long, 0.081 cm (0.032 inches) thick sheet magnesium rolled into a 20.32 cm (8 in.) diameter cylinder, which is closed with a lap-butt joint utilizing 1.9 cm (0.75 in.) wide strip magnesium bonded with Epon 934.

The inboard end cap assembly houses the two main bearings which allow the storage drum to rotate with respect to the support shaft. The constant torque negator spring motor, which provides the substrate preload force, is mounted on the inboard end cap with the output spool coaxial with the main bearings. A slip ring assembly, which functions to transfer array power signals across the rotary joint between the drums and the center support, is then mounted to the inboard end of this output spool. The outboard end cap serves as the supporting interface for the drum outer end during launch. It contains a tapered hole which mates with a tapered plug in the outboard end support. Two edge guide flanges are mounted on each storage drum to provide control forces to the substrate edge if required during retraction.

4. Center support. The center support consists of a magnesium center tube, two machined magnesium end fittings, and two magnesium face sheets. The center tube is pinned to the end fittings, and face sheets are riveted to the tube end fittings. One face sheet provides for the electrical connector installation and, together with the other face sheet, transmits shear loads. The end fittings provide the interface pads for the vehicle structure and the solar panel actuator.

5. Leading edge member. The leading edge member is the structural element on the outer-most edge of the substrate. In the deployed configuration, this member transmits the 17.8-N (4 lb) substrate preload force from the array substrates to the boom tip. In the stowed configuration, the leading edge member functions to restrain the outer substrate wrap and to cage the Bi-stem boom element.

6. Outboard end support. This arm carries the stainless steel tapered plugs which interface with the outboard end cap and leading edge member. Attachment of the movable arm to the vehicle-mounted bracket is through a hinge joint. A torsion spring which mounts on the hinge pin furnishes 1130 N-cm (100 in.-lb) of torque in the stowed configuration. The release of the support is accomplished by a separation nut/separation bolt/bolt catcher combination. The torsion spring forces the movable arm to rotate about the hinge pin through an angle of approximately 0.17 rad. The storage drum and the leading edge member are thus released to permit deployment of the solar panel actuator. The solar array structural components described above are illustrated in Fig. 2.

B. Environmental Test Program

The solar panel engineering test model was subjected to a comprehensive test program which included in summary the following tests:

(1) Deployed dynamics tests to provide necessary data on the dynamic characteristics of the deployed array. During the tests, the array was deployed vertically downward in a vacuum chamber and the system was excited with motion at the center support. Out-of plane symmetric (Z-axis), out of plane anti-symmetric (torsional) and in-plane (Y-axis) excitations were performed. Figure 3 is a photograph of an array deployed in dynamic tests.

(2) Pyrotechnic-induced shock tests to measure acceleration levels on the array components resulting from the simultaneous firing of both separation nuts (each armed with two active squibs) on the outboard end supports.

(3) Thermal-vacuum tests to measure response of the array under deployed transient, low-temperature stowed, low-temperature deploy and retract, stowed transient and high-temperature soak and high-temperature deploy and retract conditions.

(4) Acoustic noise test to monitor response of system exposed to 60 s of random incidence, reverberent sound with an overall sound pressure level of 150 dB.

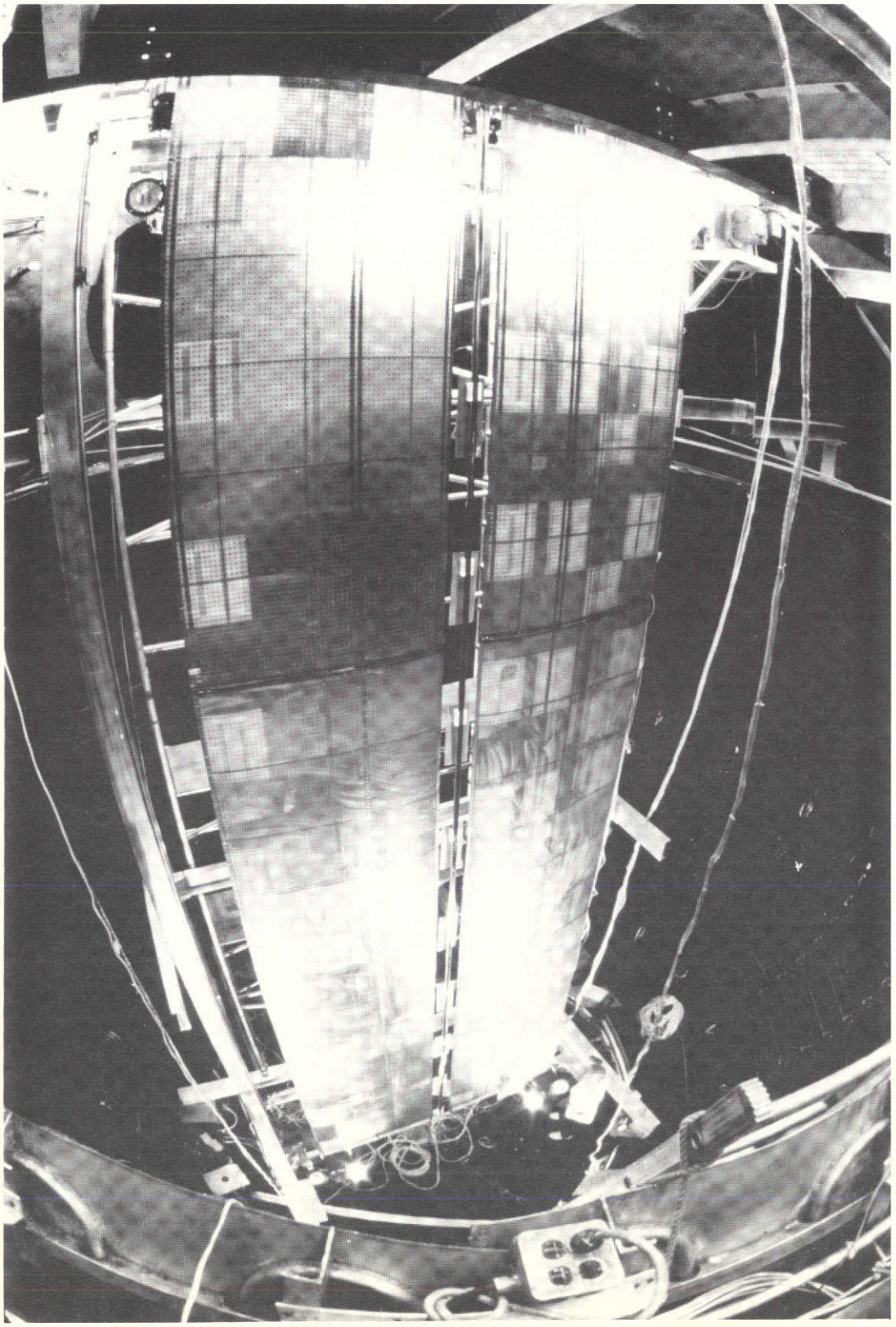

Fig. 3. 66 W/Kg Deployed Dynamics Test

(5) Stowed vibration test in Y, Z, and X-axes. The tests consisted of the following:

(a) Several 10 W-level sinusoidal sweeps.

(b) An acceptance level sinusoidal sweep at two-thirds of the specification level to evaluate linearity of system response and to provide a final assessment of risk associated with the full-level qualification input.

(c) Sinusoidal qualification sweep.

(d) Random noise testing with the same sequence (low-level, acceptance-level and qualification-level testing).

The test program, in general, achieved the major objective of providing a technology data base for this type of large area, lightweight, deployable solar array. Many test techniques applicable to other design configurations were conceived, developed and demonstrated. The most severe environment for the coverglass and solar cells was the stowed vibration test. There is no breakage pattern to indicate a possible cause for the damage. Evaluation of the cushioning material and location employed to protect cell-coverglass damage should be made for future arrays. Table 2 lists the cell and coverglass breakage resulting from the environmental tests. Table 3 summarizes the environmental tests and test levels to which the engineering test model was subjected.

Table 2. Cell and Coverglass Breakage Resulting from Environmental Test Program

Test Environment	Percent Broken Glass Platelets	Percent Broken Cells	Percent Broken Coverglass
Pyro shock	0.043	0.025	0.100
Thermal vacuum	0.213	0.400	0.825
Acoustic	0.084	0.325	0.225
Stowed vibration	0.121	0.900	1.975
35 ambient deploy/retract cycles	0.008	0.100	0.125
Total breakage	0.469	1.750	3.250

Table 3. Summary of Environmental Tests and Test Levels

Environment	Level
Pyrotechnic shock	As generated by array pyrotechnics
Thermal-vacuum tests	
Stowed	-130°C +140°C Thermal shock between -130°C and 140°C
Deployed	-130°C +140°C Thermal shock between 130°C and 140°C
Deployment	Low temp (-130°C) High temp (140°C)
Acoustic noise	150 dB overall spectrum specified
Vibration	
Sinusoidal	5-10 Hz 2.29 cm DA 10-225 Hz 4.6 g's (O-P) 225-550 Hz 0.00447 DA 555-2000 Hz 27 g's (O-P)
Random	90-700 Hz 1 G^2/Hz 20-90 Hz increasing at 6 dB/ octave 700-2000 Hz decreasing at 6 dB/ octave
Mechanical shock	250 G, 0.5 millisecond terminal sawtooth

V. APPLICATION OF GE SOLAR ARRAY CONCEPT TO SEPSIT MISSION REQUIREMENTS

A. Structural Design Considerations

1. Introduction. As described in Section III the selection of the GE rollup solar panel concept was partially based on the structural design advantages of this panel configuration, and on its extensive test history. However, it should be pointed out that in addition to the concept, a large number of component design details are also directly transferable to the larger SEPSIT panel. As a result, scaling the 2.5 kW GE panel design up to the 10 kW SEPSIT size does not appear to represent a large new development program. Some changes in the baseline GE design will be necessary, however.

Required changes in the baseline 2.5 kW design result from a number of changes in the solar panel design requirements. The most obvious change is the growth of the power requirement from 2.5 kW to 10 kW per solar panel. The space vehicle/solar panel structural interface requirements have also been updated to include our improved definition of the space vehicle attachment requirements. Similarly the mission environmental requirements have been updated for the specific launch vehicle under consideration and for the specific Encke mission flight environmental requirements.

The impact of these changes in the solar panel design requirements is discussed in the following subsections.

2. Extrapolating up to a 10 kW size panel. The primary structural change associated with adapting the 2.5 kW prototype panel to the SEPSIT space vehicle is the increased size required to meet the 10 kW power requirement. As a result of the power increase, the solar cell blanket must be approximately four times larger and thus four times heavier. This requires that the supporting structure must be stronger to survive the same launch loads with the same margin. In addition, the width of the array should increase to prevent the array from being four times longer, and thus requiring a very long and heavy boom. The length of the array and the diameter of the boom also control the natural frequencies of the deployed panel.

From the above it is clear that increasing the size of the panel presents a number of complex tradeoffs. The key parameters associated with scaling the prototype panel to the 10 kW size are the following:

(1) The width of the panel as controlled by minimizing system weight, conforming to space vehicle integration desires, and conforming to solar cell blanket width and boom actuator width requirements.

(2) The width of the solar cell blanket as controlled by conforming to overall panel width desires, minimizing circuit voltage losses, and conforming to solar cell module and bus bar spacing requirements.

(3) The lowest natural frequency of the deployed panel as controlled by the boom stiffness and length.

(4) The length and diameter of the boom as controlled by the panel length desires, lowest deployed natural frequency desires, minimum weight desires, and minimum boom development cost desires.

(5) The structural qualification test levels as determined by the launch vehicle, the space vehicle design, the solar array structural interface design, and the qualification testing and loads analysis philosophy.

In addition to the above key parameters there is the consideration as to what extent the larger SEPSIT panel should try to minimize costs by adapting to current 2.5 kW panel component designs. For example, the existing boom could be used at the expense of building a panel four times as wide as the prototype panel and accepting the corresponding factor of two reduction in deployed natural frequency. Because the drum weight would increase substantially with such a design, a more viable approach would be to try to adapt to a larger off-the-shelf boom diameter. Increasing the length of a boom requires much less development than developing a new boom diameter and its corresponding deployment mechanism.

Similar arguments apply to using some existing support structure components and accepting some redesign of others. The feasibility of using some existing prototype component designs with little or no modification is enhanced by the fact that the 2.5 kW prototype panel was designed for launch loads considerably in excess of those anticipated for SEPSIT.

3. Extrapolating to SEPSIT launch loads. The launch vibration loading occurs during boost into earth orbit and has two main components, (1) acoustic derived excitation due to interaction of the spacecraft with the surrounding acoustic noise field, and (2) launch vehicle derived excitation which is motion transmitted to the spacecraft from the launch vehicle via the spacecraft's adapter structure.

(1) Acoustic derived launch vibration

The acoustic derived excitation is generally high frequency with most excitation occurring around 300 Hz. This acoustic derived excitation generally governs the design of spacecraft components which are not part of the spacecraft's load carrying structure. Such components, like the boom actuator and the slip rings, generally have first-mode natural frequencies above 50 Hz and are strongly excited by high-frequency excitation. Acoustic derived excitation is generally considered to be random in frequency content and is specified by its power spectral density in units of g^2/Hz. The level of 1 g^2/Hz is an upper bound level for small spacecraft components and has served as the very conservative (harsh) level in the development of the 2.5 kW prototype panel.

The reason the level is very conservative for a 2.5 kW panel is that the force required to vibrate a spacecraft component increases with the component's weight. Because the excitation force is limited by the acoustic pressure forces and the strength of the component support structure, heavy components are generally subjected to lower vibration levels than small light components. As a first cut, the launch excitation level is roughly proportional to one over the square root of the component's mass. For the 2.5 kW panel no reduction was made, and the "small component" level was used directly.

For the design of the larger 10 kW SEPSIT panels it is anticipated that the random vibration qualification level will be reduced substantially, or deleted in favor of the acoustic noise test. The acoustic test was conducted on the 2.5 kW prototype panel and was found to be more representative of flight excitation.

(2) Launch vehicle derived launch vibration

Launch vehicle derived excitation is generally low frequency with the most critical excitation occurring below 50 Hz. This excitation generally governs the design of large spacecraft systems with low natural frequencies. Though the structure of small solar arrays is relatively stiff and may be sized by the acoustic derived vibration levels, large solar arrays with lower stowed natural frequencies tend to find the launch vehicle derived vibration critical. In the JPL/General Electric 66-watt/kg Rollup Solar Array program, a sinusoidal excitation of 4.6 g's (O-P) was used as the low-frequency vibration level. Because this excitation corresponds to overall launch vehicle/spacecraft vibration, subsystem mass has less effect on excitation level, and the same level is applicable to the larger 10 kW panels.

The major components excited by the low frequency excitation are the solar cell blankets and the storage drums and their supports. Only the storage drums and their supports are affected by the increased size of the 10 kW panel. The loads in these components will increase because of the increased mass of the blankets which they support.

In the design of the 2.5 kW prototype panel, the strength of the drums and support structure was determined using a very conservative (high) blanket loading. This was necessary because the complex behavior of the wrapped blankets vibrating on the drums was not amenable to normal dynamic analysis methods. During subsequent vibration testing it was observed that the blankets have a very low maximum Q. This implies that the loads are considerably less than those assumed in the design of the G. E. prototype array. As a result the components of the 2.5 kW panel may have considerable design margin and thus may require only minor redesign to handle the loads anticipated for the 10 kW panel.

(3) Low-frequency large displacement interface motion

The third type of launch loading imposed on the solar panel structure is low-frequency, large-displacement, out-of-phase interface motion. This type of motion occurs when the entire space vehicle vibrates with large amplitudes at frequencies below the first resonant frequency of the solar panel. When the solar panel attaches to the space vehicle at widely spaced interface points, the points may have significant motions relative to one another. When the space vehicle is much stiffer than the solar panel, as it must be to support the panel, these motions can create high structural loads if the panel is supported in a statically indeterminate manner. The GE rollup solar design attaches to the space vehicle at three points, in a statically indeterminate manner.

Because of its statically indeterminate support the G. E. solar panel concept requires the stiffness of the entire spacecraft structure connecting the outboard-end-supports and the center-support to be significantly stiffer than the solar panel drum/center-support assembly. In addition, low-frequency spacecraft deflection must not lead to excessive relative movement between the solar panel outboard end support and center support spacecraft interfaces.

Though the support stiffness and relative motion requirements are not too difficult to meet for the 2.5 kW solar panel, they become more significant as the width of the panel increases. To evaluate the impact of the solar panel support requirements on the SEPSIT 10 kW panels, a dynamic analysis of the combined solar array/space vehicle system was undertaken (Reference 1, Section IV-B-2). The results of the study indicate that there does not appear to be a significant problem in meeting the solar panel interface requirements. However, a sensitive area pointed out by the study is the relative motion observed between the outboard ends of the solar-panel drums and the out-board-end-support tapered plugs which engage and support the drums. This motion results in the plugs disengaging from the drums during large space vehicle deflections.

One means of correcting the above problem is to support the outboard ends of the drums on members which are fastened to, and allowed to move with the drums. This concept is sketched in Fig. 4.

In this modified out-board-end-support concept the ends of the drums are supported from the space vehicle on separable bipods. The vertex of the bipod is attached to the outboard ends of the drums with a spherical bearing and separation device. After launch the separation device is activated and the bipods swing clear of the solar panel drums. As with the original out-board-end-support design, the bipod supports also support the leading edge member and prevent the drum from unrolling during launch. The leading edge member and drum are released when the bipods swing clear. Figure 5 shows the solar panels mounted onto the SEPSIT space vehicle in the stowed (launch) configuration.

4. SEPSIT solar array configuration selection. As discussed above there are a number of structural design considerations which enter into the selection of a baseline solar array configuration. Among these are the following:

(1) Space vehicle power requirements

(2) Space vehicle configuration requirements

(3) Weight limitations

(4) Stiffness limitations

(5) Requirements for retraction

(6) Inherited technology

(7) Environmental requirements

(8) Development costs

These considerations contributed to the selection of the GE rollup array concept for the SEPSIT space vehicle. Once the GE concept was selected a number of configuration trades were performed to establish a baseline configuration. These trades made use of the extensive data acquired during the 66 watt/kg solar array development program and the parametric extrapolation

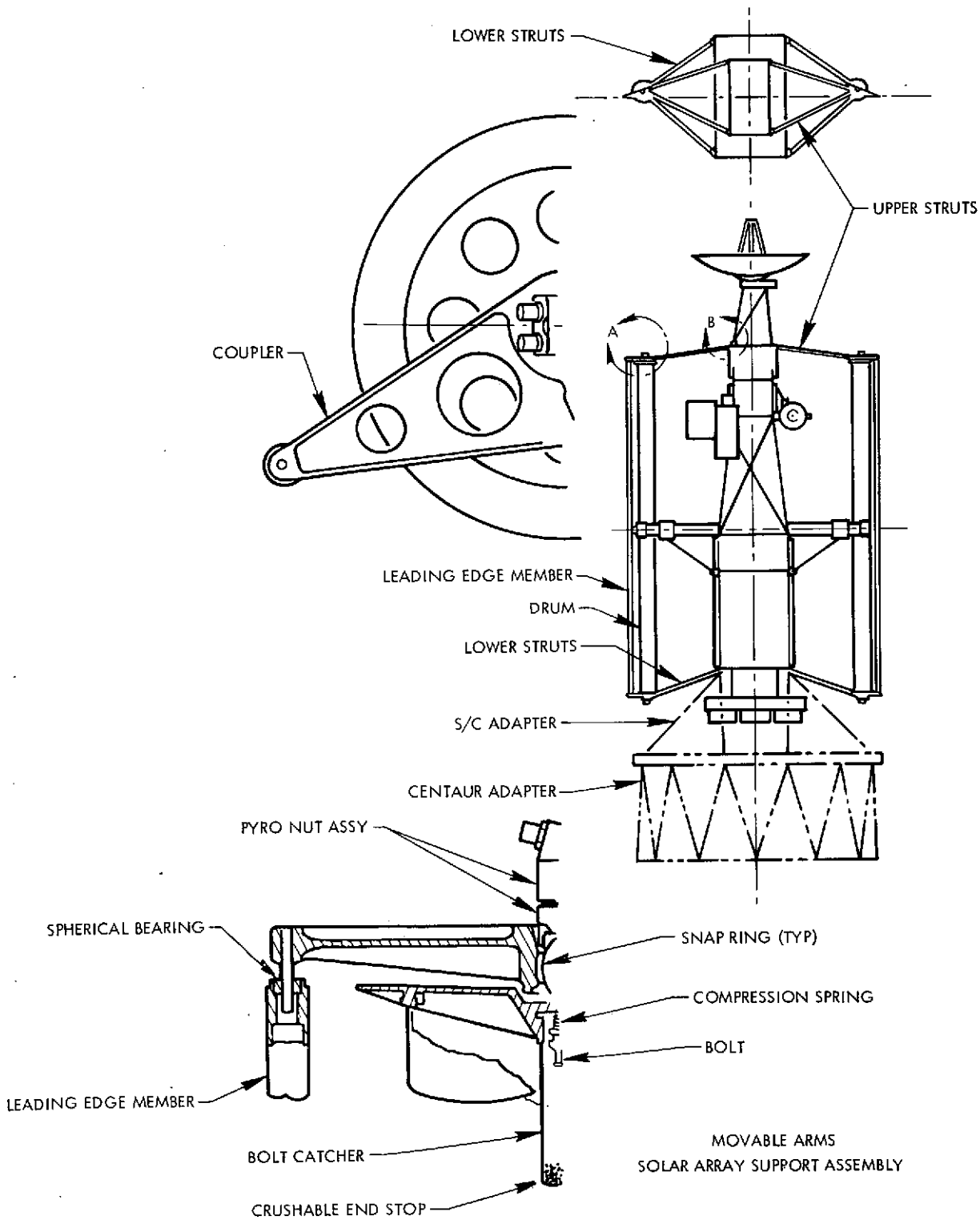

Fig. 4. Outboard End Supports

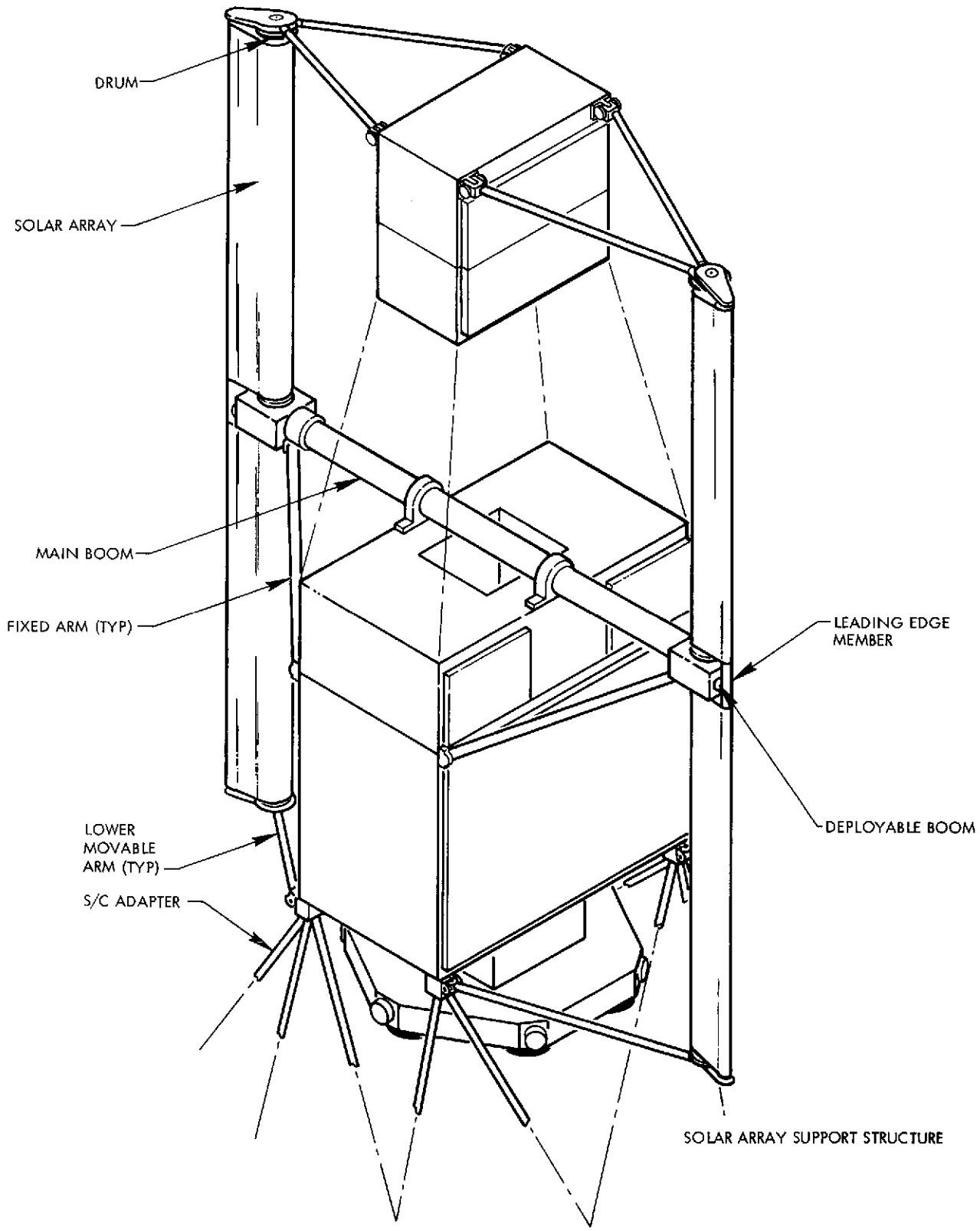

Fig. 5. Solar Panel Mounted into SEPSIT Space Vehicle in Stowed (Launch) Configuration

techniques described in Ref. 2. The extrapolation techniques were incorporated into a general purpose computer program for extrapolating from the structural performance characteristics of the prototype array to the characteristics of proposed SEPSIT array configurations (Ref. 3).

Initial trades similar to those described in Section V-B of Ref. 4 defined the minimum weight solar panel as having as low a deployed natural frequency as possible consistent with attitude control and panel fabrication requirements. This led to the selection of deployed natural frequencies in the 0.02 to 0.04 Hz range. With the desired frequency range selected, further trades established the optimum panel width for minimum weight as being in the 4 to 4.5 m (13 to 15 foot) range. This range was compatible with the spacecraft configuration and interface requirements.

Following the rough sizing, detailed solar cell and bus bar layouts were conducted as described elsewhere in this report. These layouts established the detailed dimensions of the solar cell blankets. With the blanket dimensions available, the extrapolation computer program (RUSAP) was used again to determine the minimum weight panel consistent with the deployed natural frequency requirements. During this study it was determined that the minimum deployed natural frequency was constrained to be higher than about 0.02 Hz. This constraint was imposed by the requirement that the tension in the solar cell blankets be sufficient to roll the blankets on to the drums during panel retraction. The 66 watt/kg solar array development program established the minimum tension at about 7.0 N/m (0.5 lbs/ft).

Using the minimum blanket tension requirement, the computer program determined the minimum weight boom consistent with boom buckling considerations. This was followed with an analysis of the weights of the other structural elements. The performance characteristics of the final baseline configuration of one solar panel are summarized in Tables 4 and 5.

Table 4. Deployed Array Parameters

Required power	=	10000.0 watts	
Blanket area	=	93.23 m^2	(1003.6 ft^2)
Blanket width	=	1.879 m	(6.16 ft)
Blanket length	=	24.845 m	(81.46 ft)
Array width	=	3.978 m	(13.04 ft)
Array length	=	25.150 m	(82.46 ft)
Actuator width	=	0.221 m	(0.72 ft)
Leader length	=	0.305 m	(1.00 ft)
Blanket unit wt	=	0.88 kg/m^2	(0.180 lb/ft^2)
Blanket tension	=	14.5 N/Blanket	(3.25 lb/blanket)
Applied boom load	=	0.500 of boom buckling load	
Buckling load	=	57.8 N	(13.00 lb)
Boom stiffness EI	=	3707.0 $N\text{-}m^2$	(8965.0 lb ft^2)
Boom diameter	=	0.0493 m	(1.94 in.)
Boom thickness	=	0.00025 m	(0.010 in.)
Boom unit weight	=	0.57 kg/m	(0.38 lb/ft)
Boom modulus (E)	=	0.200 + 12 N/m^2	(0.4180 + 10 lb/ft^2)
Boom matl density	=	7930.0 kg/m^2	(495.0 lb/ft^3)
Boom efficiency	=	0.80 effective (I)	
Calculated sym. freq.	=	0.018 Hz	
Calculated asym. freq.	=	0.029 Hz	

Table 5. Calculated Base Structure Parameters (Launch Acceleration = 0.50 Baseline Level)

Total blanket weight	=	83.02 kg	(182.86 lbs)
Deployed boom weight	=	14.37 kg	(31.64 lbs)
Leading edge beam weight	=	1.10 kg	(2.42 lbs)
Outboard end support assy wt.	=	5.62 kg	(12.37 lbs)
Drum shell wt.	=	8.85 kg	(19.50 lbs)
End cap + guide wt.	=	5.83 kg	(12.84 lbs)
Total drum assy weight	=	14.68 kg	(32.34 lbs)
Center support wt.	=	1.83 kg	(4.03 lbs)
Boom actuator wt.	=	7.76 kg	(17.09 lbs)
Bearing assy wt.	=	2.73 kg	(5.22 lbs)
Negator assy wt.	=	0.89 kg	(1.96 lbs)
Slipring + harness wt.	=	4.17 kg	(9.19 lbs)
Support shaft wt.	=	1.83 kg	(4.03 lbs)
Total center support assy wt.	=	18.85 kg	(41.53 lbs)
Total solar array wt.	=	137.63 kg	(303.16 lbs)
Power to weight efficiency	=	72.66 watts/kg	(32.99 watts/lb)

B. Electrical Design Considerations

1. Introduction. This section considers the parameters which influence the electrical design performance of the solar array.

The electrical characteristics of the 0.020 cm thick solar cells are described over the range of the mission environment. The rationale for the voltage range selection is discussed and a summary of the effects of the predicted solar flare proton environment for the Encke rendezvous mission on the

power output of the solar array is presented. The major sources of uncertainty associated with the prediction of array performance is examined. Performance measurement uncertainty for 3.3 AU is not considered due to the lack of available data at the present time.

Evaluation of the cabling required to achieve the electrical interconnection between each solar panel section and the slip ring harness is made and a proposed configuration is presented. The array thermal profile is discussed and in the last part of this section, the spacecraft mission trajectory assumed for power performance prediction is identified.

2. Solar cell electrical characteristics. Electrical performance parametric data was generated on 2 ohm-cm, N/P silicon solar cells, 0.020 cm (8 mil) thick, 2 cm x 2 cm, SiO coating, solderless, with Ag-Ti contacts. All data presented in this section represents the average of twelve cells.

The electrical parametric studies performed consisted of generating current voltage characteristics of the solar cells over an appropriate range of temperature-intensity. A multi-cell thermal vacuum test chamber was employed in conjunction with a solar simulator, which approximates the intensity and spectrum of space sunlight.

A Spectrolab Model X25L Mark II, close-filtered, dry nitrogen-purged solar simulator was used throughout the test program. Balloon flight standard cells comprising an intensity reference cell and separate cells having narrow-bandpass filters were mounted within the test chamber. The latter cells were used to determine the spectral quality of the solar simulator by observing its red-to-blue ratio during test.

Electrical connection to each cell was made with four wires to prevent voltage drop across the current-carrying pair from influencing the voltage reading. The solar cells are bonded to a 0.318 cm (0.125 in.) thick copper plate using General Electric RTV-560 silicon adhesive and primer. The electrical characteristics of each cell tested are obtained in the form of a current-voltage curve using a Hewlett Packard Model 7030 XY recorder. The short-circuit current and open-circuit voltage parameters are obtained on a five-place readout, integrating-type digital voltmeter. The operating temperature of the solar cells was controlled within plus or minus 0.5°C using copper-constantan thermocouples and a proportional temperature controller. The cell temperature

was varied in increments of 20 degrees between temperature extremes of plus 100 and minus 80° C.

Following the generation of the current voltage characteristics, short circuit current, open circuit voltage, current at maximum power, voltage at maximum power, and maximum power points were picked off. The current voltage curves of the twelve cells at each different test condition were averaged. Tables 6 through 10 present parametrically average values of the five parameters identified above.

3. Voltage range selection

(1) Introduction

This study was performed to determine the impact of power subsystem operating voltage upon the design, performance and reliability of the solar array, power distribution and power conditioning functions. Three voltage ranges were selected for the study: 50-100, 100-200, and 200-400 volts, because they were compatible with the voltage ranges of candidate electric propulsion power conditioners. The study also included the assessment of potential problems related to design, manufacturing, handling, testing, and component limitation. This section summarizes the results of the study and concludes with the recommendation that the 200-400 volts range be selected for the subsystem operating voltage.

(2) Results and conclusions

The results and conclusion reached in the study of each major power subsystem element are summarized below:

(a) Solar array. A rollup solar array with a voltage output between 50 to 200 volts at 1 AU, and power levels up to 10 kW can be designed and built using conventional techniques, provided that additional development effort is directed to solve problems associated with assembly, handling and testing of the large flexible array blankets. Solar array designs having output voltages of 50 to 400 volts are relatively free from the effects of space plasma in planetary missions and are substantially below the voltages that are believed to be affected by most dense regions of the ionosphere.

Table 6. Average Short Circuit Current (I_{sc}, mA)

SOLAR INTENSITY (MW/CM**2) / CELL TEMP. (DEG. C)	5.00	15.00	25.00	50.00	100.00	140.00	250.00
-80.00	3.83						
-60.00	4.29						
-40.00	4.26	11.61	21.50	40.76	84.43	114.57	210.52
-20.00	4.26	12.36	21.52	42.95	85.39	117.67	216.50
0.00	4.44	12.96	21.54	43.57	89.44	121.45	219.09
20.00	4.36	13.29	22.02	44.71	87.56	122.82	223.70
40.00	4.50	13.34	22.16	44.93	88.56	125.55	221.97
60.00	4.72	13.76	22.72	45.93	90.86	126.14	225.86
80.00							227.74
100.00							233.39

Table 7. Average Open Circuit Voltage (V_{oc}, mV)

SOLAR INTENSITY (MW/CM**2) / CELL TEMP. (DEG. C)	5.00	15.00	25.00	50.00	100.00	140.00	250.00
-80.00	722.07						
-60.00	683.25						
-40.00	632.48	667.90	677.73	695.07	709.90	715.65	718.73
-20.00	584.51	624.07	629.57	651.92	665.40	677.98	685.73
0.00	540.71	580.23	583.92	608.07	623.85	636.23	649.01
20.00	489.69	533.23	537.07	561.67	574.23	594.15	607.07
40.00	439.65	484.40	491.57	517.19	533.57	547.37	563.20
60.00	391.31	434.40	442.23	470.30	486.23	502.49	516.57
80.00							473.82
100.00							429.24

Table 8. Average Maximum Power Current (I_{mp}, mA)

SOLAR INTENSITY (MW/CM**2) / CELL TEMP. (DEG. C)	5.00	15.00	25.00	50.00	100.00	140.00	250.00
-80.00	3.25	-0.00	-0.00	-0.00	-0.00	-0.00	-0.00
-60.00	3.87	-0.00	-0.00	-0.00	-0.00	-0.00	-0.00
-40.00	3.71	10.50	19.53	38.56	81.91	110.83	203.35
-20.00	3.72	11.07	19.73	39.76	79.83	113.25	204.58
0.00	3.91	11.70	19.61	40.84	82.17	113.42	206.25
20.00	3.86	11.92	20.30	41.72	80.75	114.63	205.58
40.00	3.93	12.01	19.67	41.80	81.33	117.04	204.50
60.00	4.14	12.20	19.48	41.49	81.00	116.25	203.42
80.00	-0.00	-0.00	-0.00	-0.00	-0.00	-0.00	202.67
100.00	-0.00	-0.00	-0.00	-0.00	-0.00	-0.00	206.50

Table 9. Average Maximum Power Voltage (V_{mp}, mV)

SOLAR INTENSITY (MW/CM**2) / CELL TEMP. (DEG. C)	5.CC	15.0C	25.C0	50.00	100.C0	140.00	250.00
-8C.CC	618.33	-0.CC	-C.C0	-0.00	-C.00	-0.00	-0.00
-6C.CC	586.67	-0.CC	-C.00	-0.00	-0.C0	-0.00	-0.00
-4C.CC	53C.83	591.67	600.C0	612.08	608.33	613.75	600.83
-2C.C0	475.83	551.67	545.C0	567.92	575.00	579.00	573.33
C.CC	444.17	5C1.67	498.33	521.67	535.00	545.00	539.17
2C.CC	4C4.17	458.33	450.C0	470.42	478.33	500.83	498.33
4C.CC	362.5C	413.33	401.67	428.33	425.C0	442.67	446.67
6C.CC	3C3.33	365.CC	350.00	387.50	390.00	404.17	404.17
8C.CC	-C.CC	-0.CC	-C.00	-0.00	-0.00	-0.00	362.50
1CC.CC	-C.CC	-0.0C	-0.00	-0.00	-0.00	-0.00	314.17

Table 10. Average Maximum Power (P_{max}, mW)

SOLAR INTENSITY (MW/CM**2) / CELL TEMP. (DEG. C)	5.00	15.00	25.00	50.00	100.00	140.00	250.00
-80.00	2.02	-0.00	-0.00	-0.00	-0.00	-0.00	-0.00
-60.00	2.27	-0.00	-0.00	-0.00	-0.00	-0.00	-0.00
-40.00	1.98	6.21	11.72	23.55	49.83	68.01	122.12
-20.00	1.77	6.12	10.76	22.64	45.90	65.57	117.34
0.00	1.74	5.88	9.78	21.27	43.96	61.83	111.19
20.00	1.55	5.47	9.13	19.62	38.62	57.35	102.38
40.00	1.42	4.93	7.90	17.92	34.56	51.77	91.34
60.00	1.25	4.45	6.82	16.09	31.59	46.98	82.18
80.00	-0.00	-0.00	-0.00	-0.00	-0.00	-0.00	73.50
100.00	-0.00	-0.00	-0.00	-0.00	-0.00	-0.00	64.92

Calculation of the solar array design based on the GE engineering model has shown that the specific power density (watt/kg) is greater at the highest voltage design of 200 to 400 volts for all power levels. The data obtained are summarized in Table 11.

(b) Power distribution system. Analysis of the power distribution determined that the least power loss and the least weight are obtained within the design voltage range of 200 to 400 volts. The data obtained are summarized in Table 12.

(c) Pre-regulator and propulsion housekeeping. The pre-regulator efficiency calculations show that the efficiency is somewhat higher within the input voltage range of 100 to 200 volts. However, the power processed by the pre-regulator is less than 4% of the total solar array power generated and processed and has little overall design impact.

The pre-regulator and inverter designs are considered to be essentially state-of-the-art over the entire voltage range of 50 to 400 volts. The study assumed that high voltage transistors are available and would be qualified and accepted.

4. Radiation study. In this section the effects of the predicted solar flare proton environment for the Encke Rendezvous (1980) Mission on the power output of the SEPSIT Solar Array are considered. Figures 6, 7, 8, 9, and 10 define the predicted solar flare environments. These curves define probabilities of encountering fluences of solar flare protons having kinetic energies greater than 10, 30, and 100 MeV. The environment is independent of direction of incidence. The probability values presented are the probabilities that the fluence will exceed Fluence (F) at energies greater than Energy (E). Figures 6 through 10 were used to generate log-log plots of fluence $\phi(>E)$ versus proton energy with days from launch and probability as parameters. The equivalent 10 MeV proton fluence was calculated according to:

$$10\ \text{MeV} = \sum_{E=0}^{\infty} \left[\phi(>E) - \phi(>E + \Delta E) \right] \cdot D(E, t)$$

Table 11. Solar Array Voltage and Power Density

Power Output in Watts/Panel	Launch Acceleration g's	Voltage at 1AU		
		50V	100	200
		Power Density Watt/kg	Power Density Watt/kg	Power Density Watt/kg
2.5 kW	9.0	66.8	67.60	68.2
2.5 kW	4.5	81.2	82.18	82.9
5.0 kW	9.0	53.3	53.9	54.7
5.0 kW	4.5	70.1	70.9	71.9
10.0 kW	9.0	42.8	43.4	44.0
10.0 kW	4.5	56.6	57.5	58.1

Table 12. Voltage Range and Weights Analysis of the Power Distribution System

Voltage Range	Power Generated/Dist.	"Least Weight" Design		"Least Power Loss" Design	
		Weight Kg	Losses Watts	Weight Kg	Losses Watts
50-100 V	20 kW/16 kW	64.6	874.0	78.6	735.0
100-200 V		36.8	555	50.0	349.0
200-400 V		30.8	293	42.9	143.0

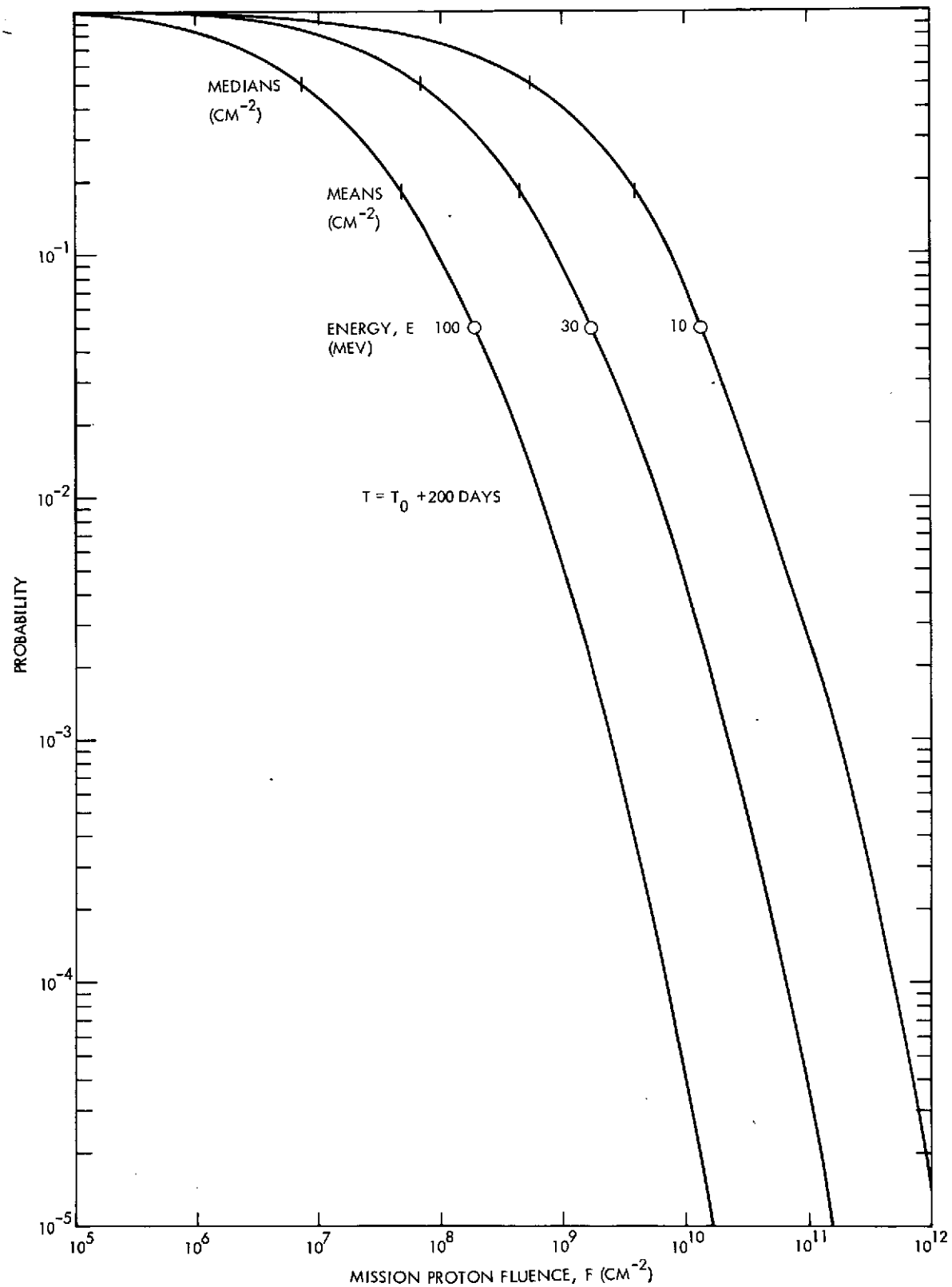

Fig. 6. Predicted Solar Flare Environment 200 Days Following Launch

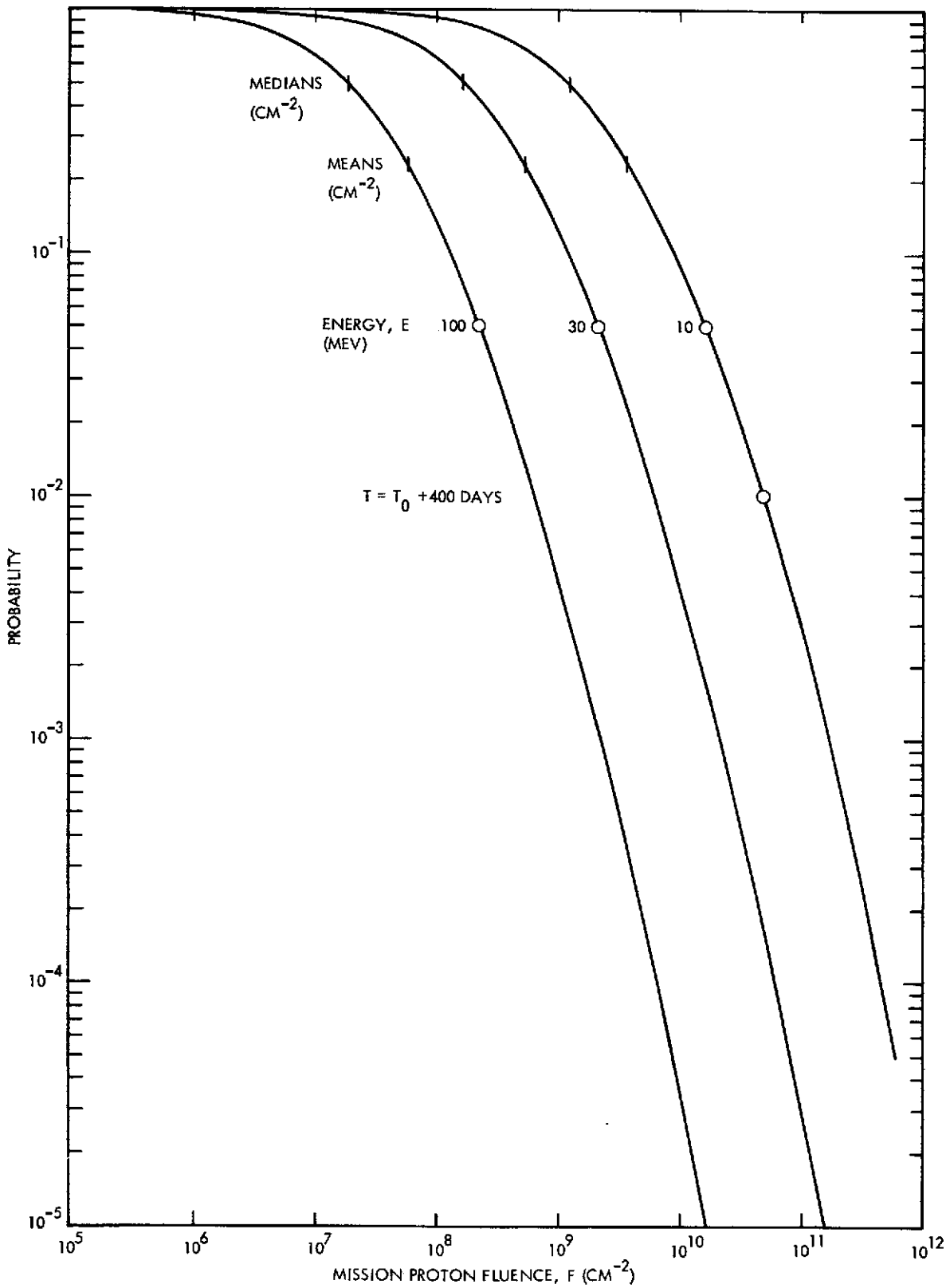

Fig. 7. Predicted Solar Flare Environment 400 Days Following Launch

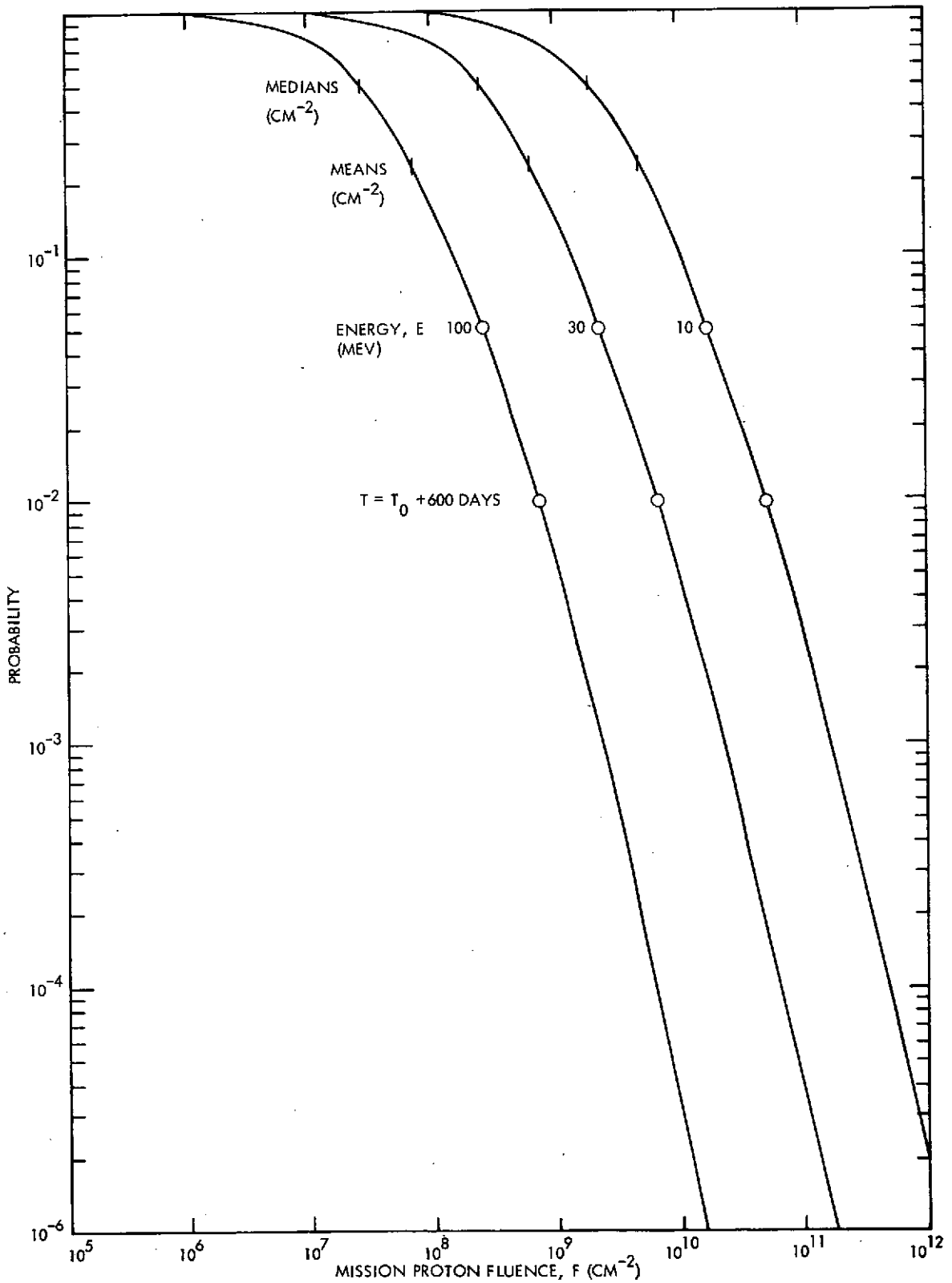

Fig. 8. Predicted Solar Flare Environment 600 Days Following Launch

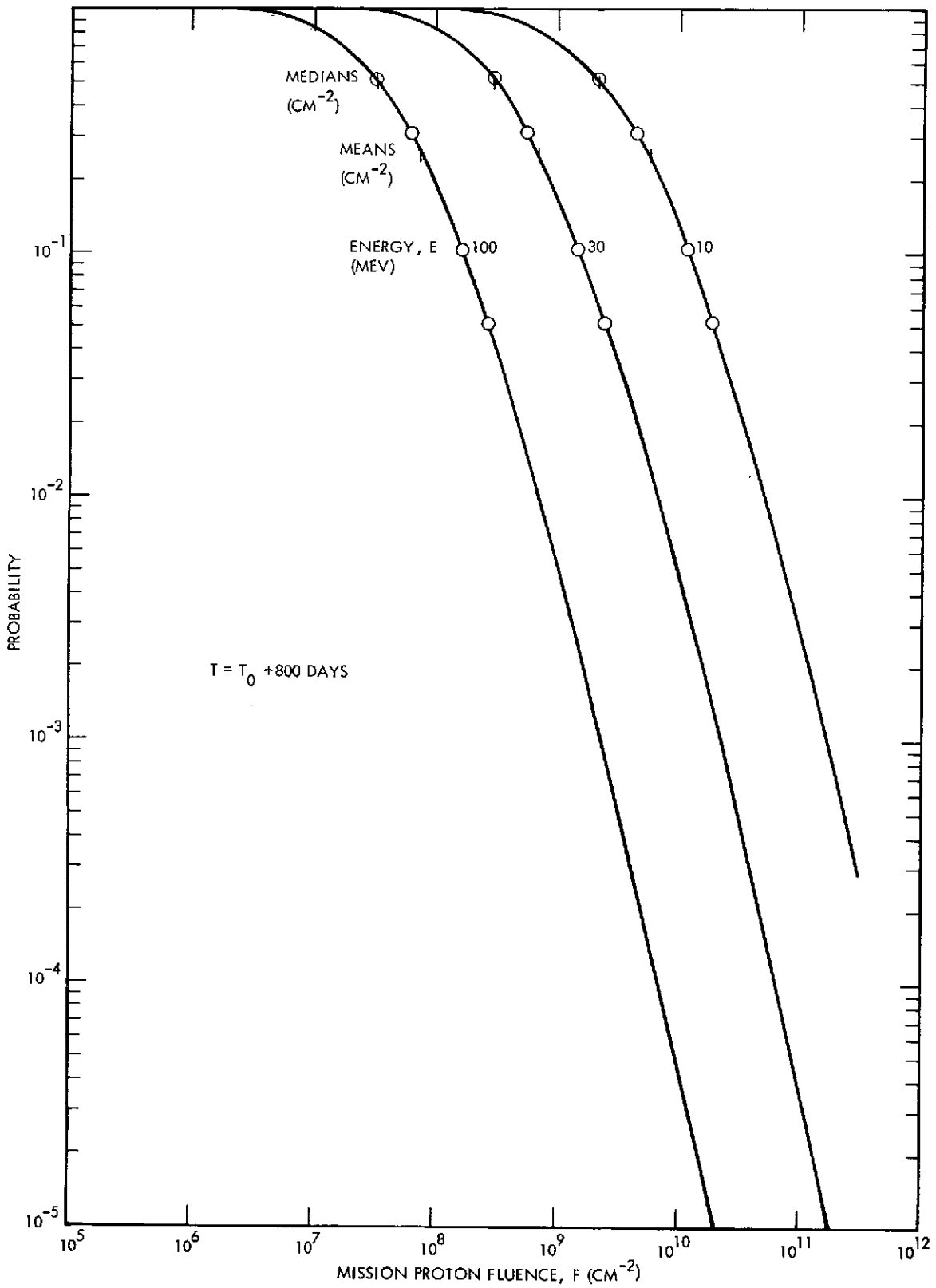

Fig. 9. Predicted Solar Flare Environment 800 Days Following Launch

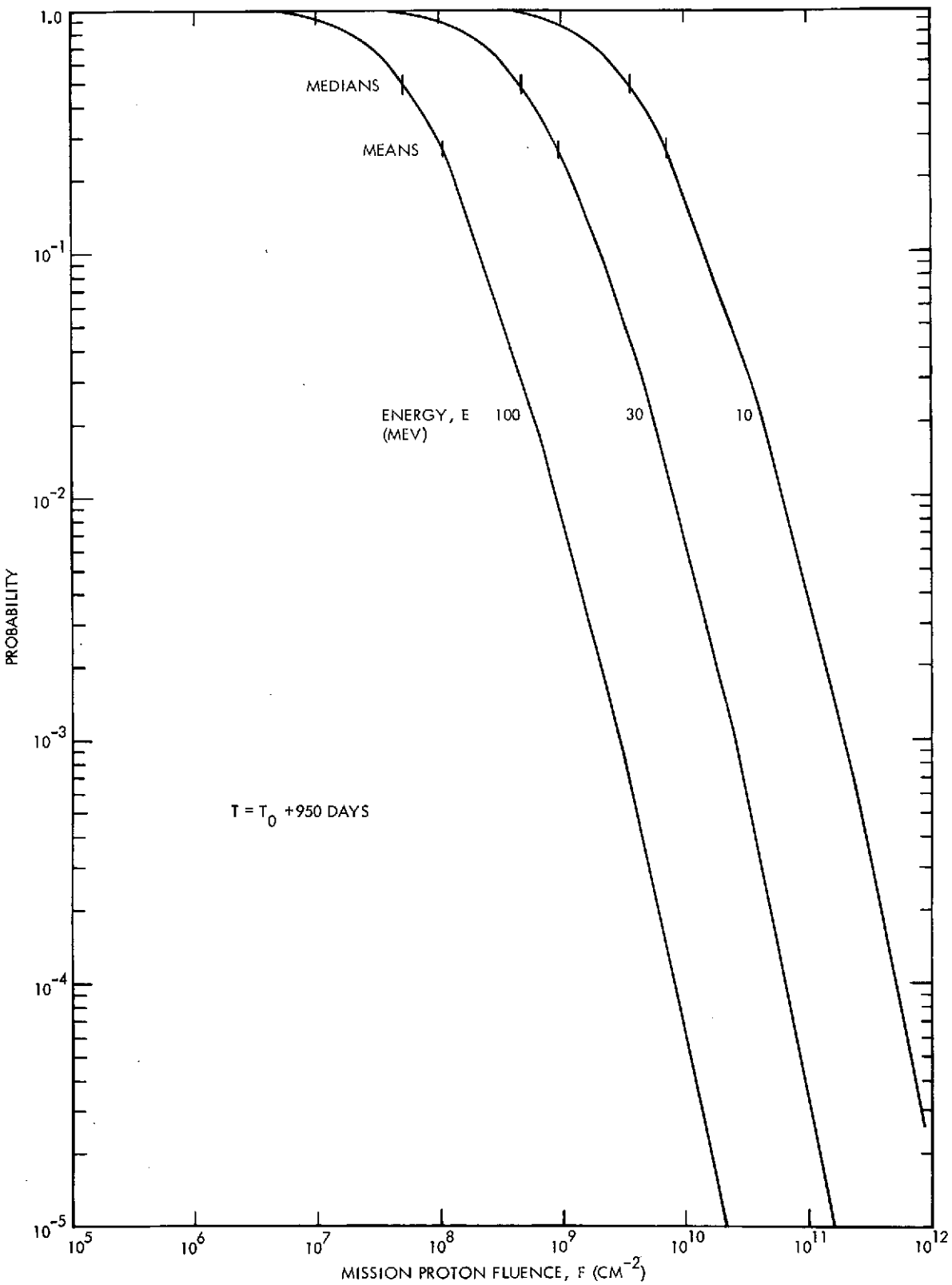

Fig. 10. Predicted Solar Flare Environment 950 Days Following Launch

where

$10\ \text{MeV}$ = The damage equivalent 10 MeV proton fluence

$\phi(>E) - \phi(>E + \Delta E)$ = The isotropic proton fluence having energies in a small energy increment greater than energy E.

$D(E,t)$ = The relative damage coefficient for isotropic fluences of protons of energy E on solar cells shielded by cover glass of thickness t.

The log-log plot discussed above is used to determine $\phi(>E) - \phi(>E + \Delta E)$. $D(E,t)$ as well as a thorough discussion of the degradation calculation method used in this study can be found in Ref. 5. The equivalent 1 MeV electron fluence was estimated according to:

$$1\ \text{MeV e} = 10\ \text{MeV p} \times 3000$$

The 1 MeV electron fluence was determined for a 0.020 cm cell and 0.008 cm coverglass. Equivalent 1 MeV electron fluence data was converted to power degradation using power vs fluence curves found in Ref. 5. A summary of the radiation calculations is presented in Fig. 11 where maximum power degradation is plotted as a function of time following launch with probability as a parameter. Probabilities of 50, 70, 90, and 95% were considered.

The following example illustrates how the curves should be interpreted. Consider the point 950 days following launch on the 50% probability curve. $P/P_0 = 0.92$ at this point. Array degradation is expressed as $((1-P/P_0) \times 100\%)$. Thus, there is a 50% probability that the array degradation will be 8% or less at 950 days following launch. These calculations are based on infinite back shielding. In reality the back shielding is not infinite and is approximately three times the thickness of the front shielding. The effect of the non-infinite back shielding is to increase the array degradation considering infinite back shielding by about 10%. Thus the effect on the example discussed above would be about 0.8%.

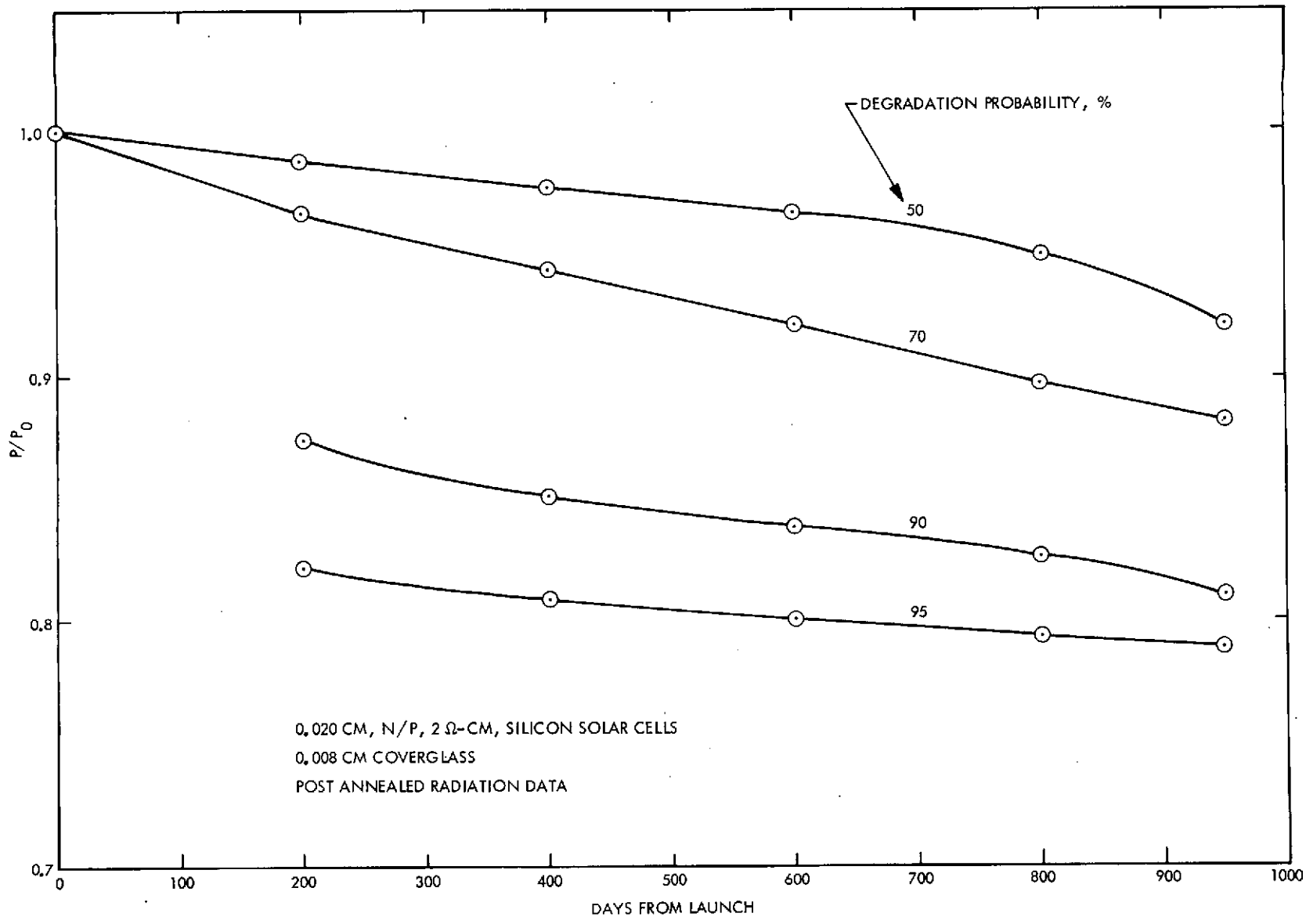

Fig. 11. Maximum Power Degradation as a Function of Time Following Launch with Probability as a Paremeter

5. Uncertainty. This section examines the major sources of uncertainty and error in predicting the post launch electrical performance of the array. The analysis method used was developed by Anspaugh (Ref. 6).

Using the JPL M132000 computer program to predict the panel output, an uncertainty in the prediction of I_{sc}, V_{oc}, and P_m follows:

$$\left(\frac{dI_p}{I_p}\right)^2 = \left(\frac{dH}{H}\right)^2 + \left(\frac{\alpha_0\, dT_t}{I_t}\right)^2 + \left(\frac{n\alpha\, T_p}{I_p}\right)^2 + \left(\frac{dI}{T}\right)^2_{TM} + S_I^2 + e_I^2 \tag{1}$$

$$\left(\frac{dV_{oc}}{V_{oc}}\right)^2 = \left(\frac{1}{V_{oc_t}} \frac{dV_{oc_t}}{dT}\, dT_t\right)^2 + \left(\frac{1}{V_{ocp}} \frac{dV_{oc_t}}{dT} dT_p\right)^2 + \left(\frac{1}{V_{oc_p}} \frac{dV_{oc}}{dH}\, \beta dH\right)^2$$

$$+\left(\frac{dV_{oc_p}}{V_{oc_p}}\right)^2_{TM} + S_v^2 + e_v^2 \tag{2}$$

$$\left(\frac{d\, P_m}{P_m}\right)^2 = \left(\frac{dV_{oc}}{V_{oc}} \frac{V_{oc}}{V_{mp}}\right)^2 + \left(\frac{dI_{sc}}{I_{sc}} \frac{I_{sc}}{I_{mp}}\right)^2 \tag{3}$$

The terms appearing in the above equations are defined below:

I_p = panel current, mA

I_t = single cell current, mA

H = solar intensity at which solar cell output is predicted, mW/cm

dH = solar intensity uncertainty including simulator intensity uncertainty when the parametric solar cell data used in M132000 was acquired and the uncertainty of the solar intensity incident on the spacecraft.

α_0 = temperature coefficient of short circuit current at the nearest tabulated (H, T) point in M132000 to the desired intensity and panel temperature, $m\lambda/°C$.

α = same as α_0, but at the desired intensity and panel temperature

dT_t = cell temperature uncertainty during parametric data acquisition °C

dT_p = panel temperature uncertainty, °C

n = number of cells in parallel on the panel

$\left(\frac{dI}{I}\right)_{TM}$ = uncertainty in measuring solar panel current at Table Mountain

S_I = statistical 95% confidence limit of the parametric current data, mA

e_I = current prediction error of M132000, mA

V_{oc_p} = panel open circuit voltage, mV

V_{oc_t} = single cell open circuit voltage, mV

$\left(\frac{dV_{oc_p}}{V_{oc_p}}\right)_{TM}$ = uncertainty in measuring the solar panel voltage at Table Mountain

S_v = statistical 95% confidence limit of the parametric voltage data, mV

e_v = voltage prediction error of M132000, mV

P_m = panel maximum power, mW

V_{mp} = voltage at maximum power, mV

I_{mp} = current at maximum power, mA

Values for the terms appearing in Eqs. (1) and (2) are summarized in Table 13. These values are appropriate for an incident solar intensity of 140 mW/cm^2

Table 13. Values for SEPSIT Solar Array Performance Prediction Uncertainty Calculation @ 140 mW/cm^2, 52°C

$\frac{dH}{H} = 0.015$	
$\alpha_0 = 0.09$ mA/cm^2	$\frac{dV_{oc_t}}{dT} = 2.28$ mV/°C
$dT_t = \pm 1$°C	$\frac{V_{oc_p}}{m} = 522$ mV
$I_t = 126$ mA	$\frac{dV_{oc_t}}{dH} = 0.25$ mV/mW/cm^2
$\frac{I_p}{n} = 126$ mA	$dH = 2.1$ mW/cm^2
$dT_p = \pm 5$°C	$\left(\frac{dV_{oc_p}}{dV_{oc_p}}\right)_{TM} = 0.012$
$\left(\frac{dI}{I}\right)_{TM} = 0.0115$	
$S_I = 0.017$	$S_v = 0.86$
$e_I = 0.0136$	$e_v = 0.78$
$V_{oc_t} = 522$ mV	

(1 A.U.) and a solar panel temperature of 52°C and when substituted in Eqs. (1) and (2) give the following values of uncertainty:

$$\frac{dI_{sc}}{I_{sc}} = \mp 2.94\%$$

$$\frac{dV_{oc}}{V_{oc}} = \mp 2.78\%$$

The total uncertainty in the array maximum power can be computed using Eq. (3). For the SEPSIT solar array at 1 A.U. and 52°C the following values are appropriate:

$I_{sc} = 95.2$ Amps

$I_{mp} = 84.5$ Amps

V_{oc} = 270.3 Volts

V_{mp} = 214.8 Volts

Substituting the above values for I_{sc}, I_{mp}, V_{oc}, and V_{mp} together with the values for the current and voltage uncertainties into Eq. (3) gives the following array maximum power uncertainty:

$$\frac{dP_{max}}{P_{max}} = \pm 4.8\%$$

6. Cabling Interconnection Study. The purpose of this study is to make a preliminary investigation of various cabling methods to achieve the electrical interconnection between each solar panel section and the drum slip ring harness.

(a) Cabling Assembly Constraints

(1) Each of the 12 sections is to have an electrically independent cabling subsystem running from the section to the slip ring.

(2) Power loss in each subsystem shall be limited to a maximum of two (2) percent of the nominal power generated by each section, at 1 AU.

(3) The voltage drops over the subsystem cables shall be such that the voltages at the slip ring interface shall be equal for each section.

(4) The cabling shall be sufficiently flexible to not adversely affect the deployment of the solar panels.

(b) Cable-Section Interconnection

Two approaches were investigated for connecting the electrical panel sections to the slip ring harness. The first approach considers the connection to be made at the end of the electrical section (Fig. 12), the area nearest the slip ring, to minimize the cable length required. The second approach considers the electrical connection at the mid-point of the electrical section as shown in Fig. 13.

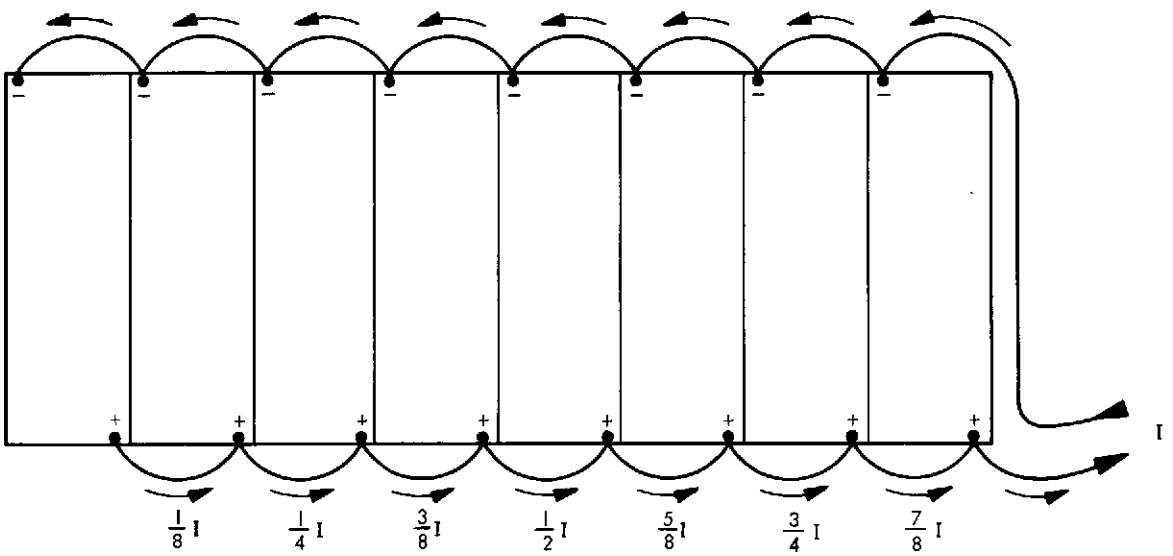

Fig. 12. Current Flow in Section Jumpers — End Connection

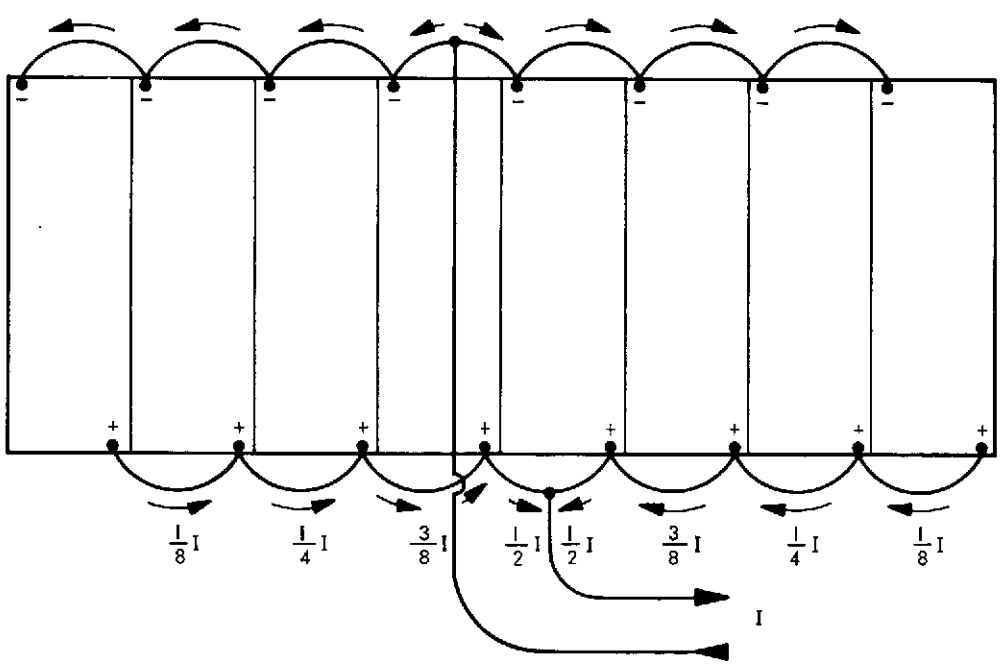

Fig. 13. Current Flow in Section Jumpers-Midpoint Connection

Since the eight (8) subsections within the individual sections are identically configured and are jumpered together in parallel, the conductors (jumpers in all subsections) would be sized for the maximum current flow of the generated current of a subsection for the end connection scheme. To reduce the current flow in the conductor and allow a corresponding decrease in conductor size, the electrical connection at the mid-point is the preferred approach. Furthermore, the constraint associated with maintaining equal voltage drops for each section introduces a problem when utilizing an electrical interface at the end of the section. The allowable power dissipation assuming a maximum power output of 1625 watts per section is Pd = 0.02 × 1625 = 32.5 watts.

$$\text{The cable loop resistance } Re = \frac{32.5}{(7.17)^2} = 0.632 \text{ ohm}$$

$$\text{or one way } \frac{0.632}{2} = 0.316 \text{ ohm}$$

In other words, for the same I_{mp} current, the one way resistance of the cable from each section to the slip ring is 0.316 ohm. Because of extremely small distances from the nearest corner of the adjacent section to the slip ring, as compared to the outboard sections, a resistance of this value will be required. Rather than designing the cable for this resistance value to maintain equal voltage drop for the sections, it is suggested that this cable should be fabricated using the same material as the copper conductors of the other cables and an auxiliary resistor added in series to the inboard section circuit.

Connection at the mid-point of the electrical section provides the following advantages:

(1) Reduced current flow in the subsection jumper conductors of 1/2 maximum section current.

(2) Provides symmetrical thermal gradients over the section and

(3) Provides symmetrical current which cancels the overall magnetic fields for each section.

It is proposed to use six (6) separate and insulated 2.9464 mm (0.116 inch) wide conductors, parallelled at each end to achieve the required resistance. This design provides advantages such as the thermal dissipation is spread over a large area; the 2.9464 mm (0.116 inch) conductor is readily available and the direction of current flow can be reversed in adjacent conductors providing

magnetic field cancellation. The proposed configuration is shown in Fig. 14 where two 0.8890 mm (0.035 inch) temperature transducer lines are included in the "to" and "from" cables required to interconnect each section.

As shown in Fig. 13 the complete cable assembly for each section consists of 2 identical cables. These will be separate, i.e., not bonded. Spot bonds could be employed along the length so that the amount of separation could be controlled without causing stresses on the conductors.

The analysis above is based on the longest cable run to the mid-points of the farthermost section. To achieve the same resistance to the mid-point of the center sections which have a cable run of approximately 12.4358 m (40.8 ft), only 4 parallel conductors of 2.4130 mm (0.095 inch) width with the same thickness would be required. The closest sections to the slip ring harness require only one 2.9464 mm (0.116 inch) wide conductor to the midpoints. If it is desired to have 2 conductors in parallel for redundancy, then the widths could be halved. Detailed analysis of the cabling requirements appears in Reference 7.

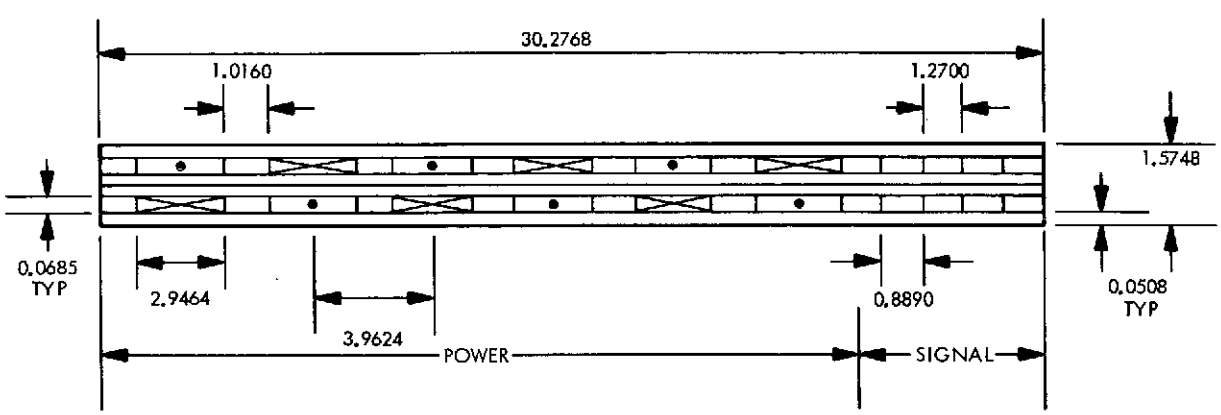

NOTE: DOTS AND CROSSES DENOTE CURRENT FLOWS OUT OR INTO THE PLANE OF THE PAPER RESPECTIVELY FOR MAXIMUM MAGNETIC FIELD CANCELLATION.

DIMENSIONS ARE IN MILLIMETERS

Fig. 14. Proposed Flat Cable Assembly

7. Thermal Analysis. The thermal analysis of the solar panels is complicated by the fact that the SEPSIT cell blanket contour cannot be predicted with great certainty. However, prior JPL experience with rollup panels strongly suggests that the blanket contour, neglecting geometrical edge effects along the drum and along the leading edge member, can be approximated by the so-called one-dimensional edge curl model shown in Fig. 15. The cross section of the blanket model through a row of cells is regarded to be a circular arc; whereas, the cross section through a column of cells would appear as a straight line.

If the thermal edge effects and conduction are neglected, the temperature along a column of cells is constant. The relationship between the temperature of cell column i and the temperatures of the other cell columns is given by the steady-state heat balance for column i, that is:

$$q_1 + q_2 + q_3 = q_4 + q_5 \tag{4}$$

where q_1 = solar flux absorbed by direct solar incidence,

q_2 = solar flux absorbed as a result of reflections from other cell columns,

q_3 = infrared flux absorbed due to thermal emission from other sources such as cell and spacecraft reflections,

q_4 = infrared flux emitted by front (cell/coverglass) and back (substrate) sides of cells in column i,

q_5 = electrical power per unit area of column i extracted by spacecraft electrical load.

The above expression neglects the conductive coupling (a conservative assumption) which exists between cells by virtue of the electrical connections and the cell substrate.

The mathematical equivalent of Equation (4) is:

$$\alpha S \max(\cos\theta_i, 0) + \sum_{j=1}^{N} \alpha\rho G_{j,i} S \max(\cos\theta_j, 0) + \sum_{j=1}^{N} \epsilon(t_i)\, \epsilon(t_j)\, F_{j,i}\, \sigma T_j^4$$

$$= \left[\epsilon(t_i) + \epsilon_s(t_i)\right] \sigma T_i^4 + (P/A)_o\, R_i\, \psi(R_i)\, \Phi(t_i) \tag{5}$$

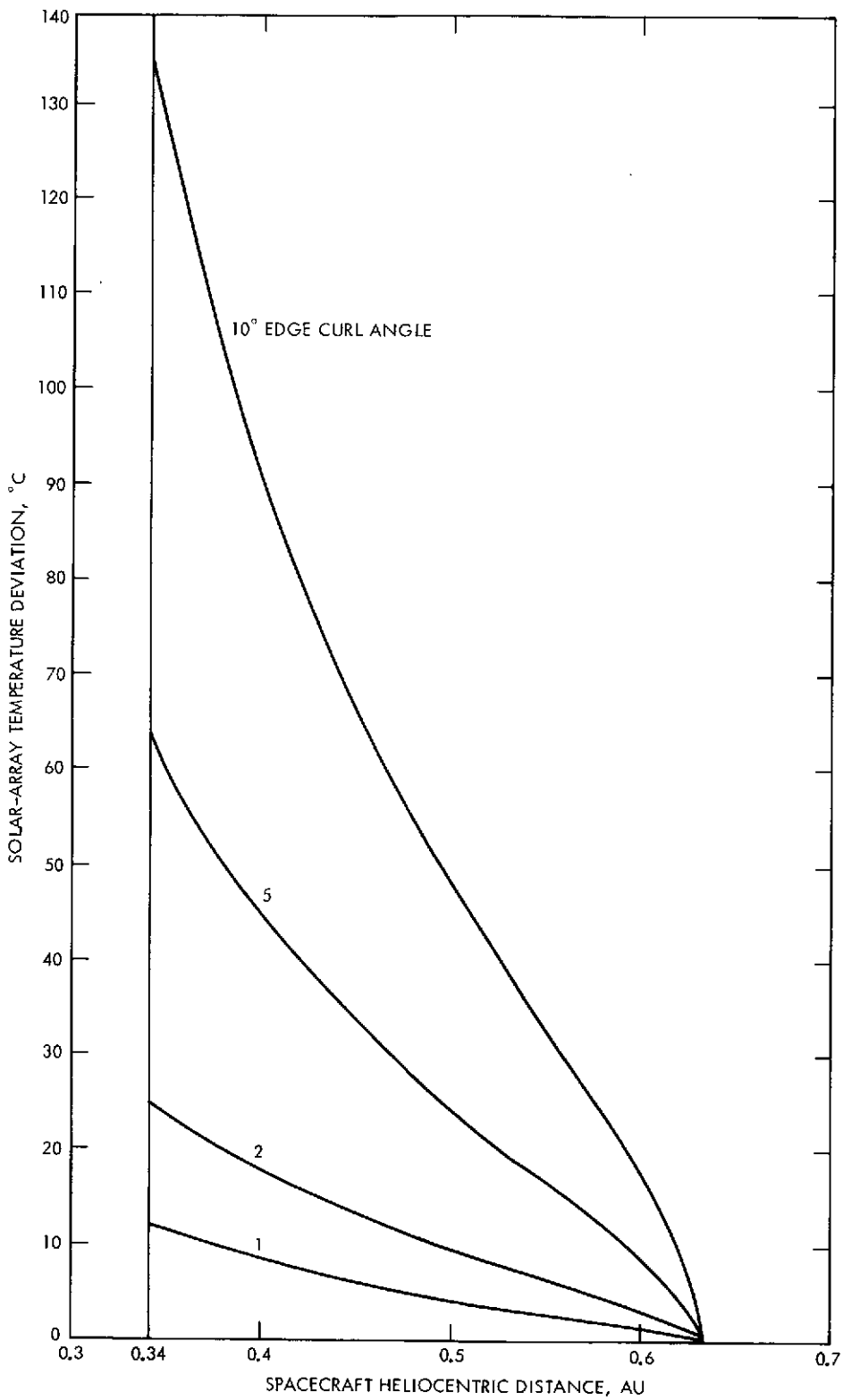

Fig. 15. Effect of Edge Curl on Solar-Array Temperature

where T = absolute temperature, K

t = temperature, °C

α = solar absorptance of cell/coverglass

ρ = solar reflectance of cell/coverglass = $1 - \alpha$

ϵ = emittance of cell/coverglass, function of t

ϵ_s = back side (cell substrate) emittance, function of t

$F_{j,i}$ = infrared form factor from column j to column i

$G_{j,i}$ = solar form factor from column j to column i

σ = Stefan-Boltzmann constant

S = local value of solar irradiance

θ = angle between cell area normal and a solar ray

R = effective relative irradiance = $\frac{S}{S_e} \max(\cos\theta, 0) \frac{1-r(\theta)}{1-r(0)}$

r = effective reflectance of coverglass (estimated by the Fresnel formulas and Snell's law for fused silica), function of θ

ψ = cell relative efficiency, function of R

Φ = cell relative efficiency, function of t

$(P/A)_o$ = solar cell electrical power output per unit area for R=1 and t = 60°C

N = number of cell columns

and subscripts i, j, and $\oplus$ denote column i, column j, and earth, respectively.

Equation (5), in reality, represents a system of non-linear, simultaneous equations (since the index i can run from 1 through N). It should be noted, however, that the equations become uncoupled if q_2 and q_3 (the second and third terms, respectively) vanish as they do when the blankets are flat. To determine the effect of these terms, solutions were obtained with q_2 omitted and with q_2 included with $G_{j,i}$ matrices spanning the range of fully specular to fully diffuse solar reflections. The test was then repeated with q_3 omitted. For edge curl angles of 10 degrees or less, the net effect of q_2 and q_3 amounted to only a few degrees C. On the basis of this information, subsequent calculations were simplified considerably by omitting these terms.

For the purpose of this analysis, the pertinent thermophysical and electrical properties of Mariner '71 cell/filters were assumed. These data, obtained from JPL TM 33-473, are regarded to be representative for the type of cell/filter which may ultimately be selected. The General Electric, 66 watt/kg, rollup panel prototype, for example, utilized an 0.020 cm, N/P, 2 ohm-cm cell with an unfiltered, 0.020 cm coverglass. A flight version would probably use a coverglass equipped with a #415 blue filter. Except for the thickness of its components, the Mariner '71 cell/filter combination is identical.

The panel blanket substrate used in the thermal model is Kapton. Cells are assumed to be bonded onto the substrate with G.E. SMRD-745 adhesive. Test data indicates that the emittance for the substrate/adhesive combination can be estimated by

$$\epsilon_s(t) = 0.74 - \frac{0.02}{123}(t-27).$$

Working under the assumption that only soft-solder interconnect technology will be used for the construction of the rollup panels, reliability considerations suggest the adoption of 140°C as the maximum permissible solar cell blanket temperature. The simplest temperature control scheme is to rotate the panels about their longitudinal axis, when necessary, so that the cells are exposed to solar rays at something less than normal incidence.

The results of the analysis are summarized in Figs. 16 and 17. In Fig. 16, it is seen that solar panel rotation is not required at heliocentric distances greater than 0.635 AU since the average panel temperature will be less than 140°C. But for lesser heliocentric distances, the required angle of rotation rapidly increases to 73.4 degrees at perihelion (0.34 AU). Edge curl effects do not become significant until the solar panels are rotated. Thus, only the results for heliocentric distances of less than 0.635 AU are shown. At greater distances, temperature deviations amount to less than 2°C for edge curl angles of up to 10 degrees.

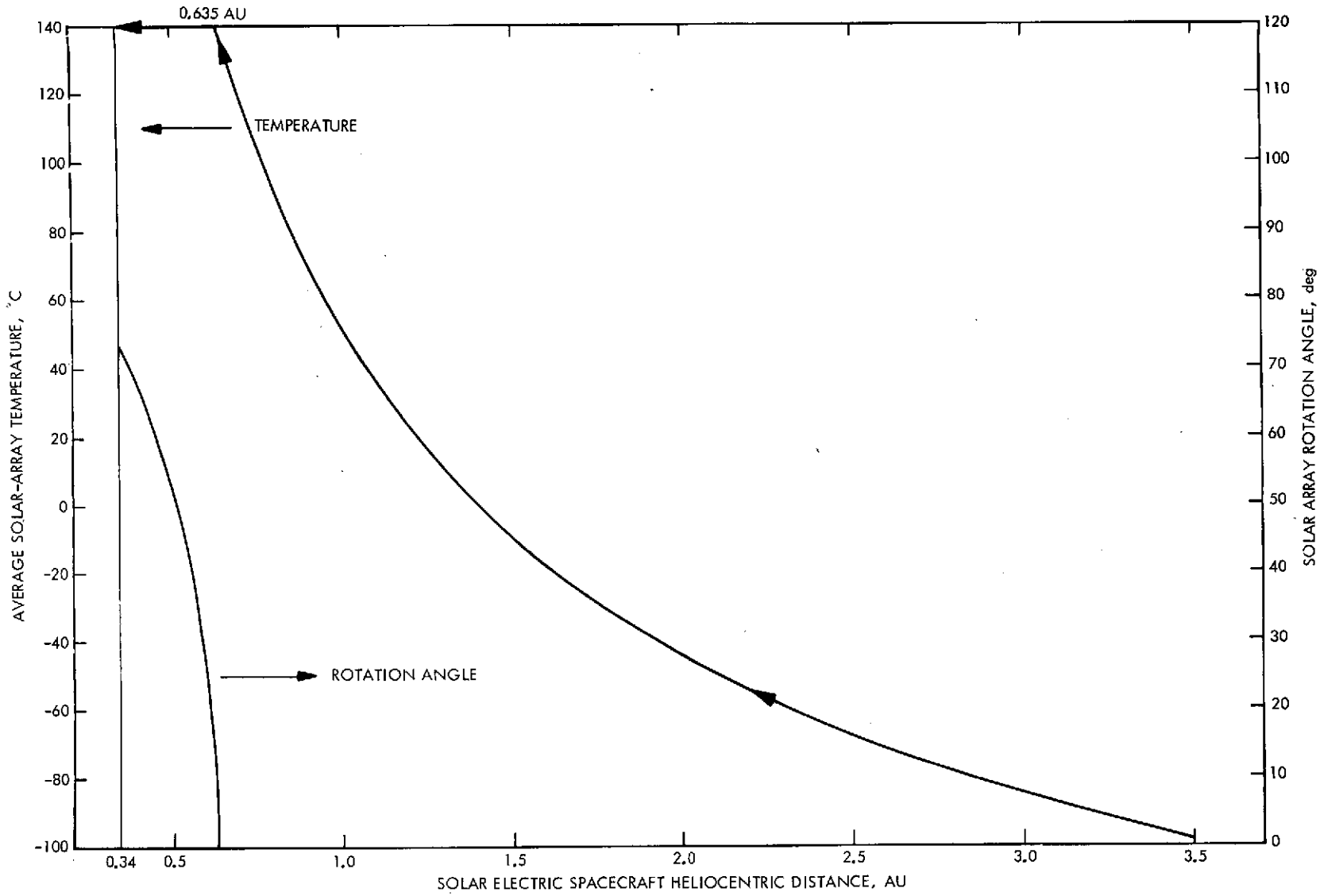

Fig. 16. Solar-Array Sensitivity to Heliocentric Distance

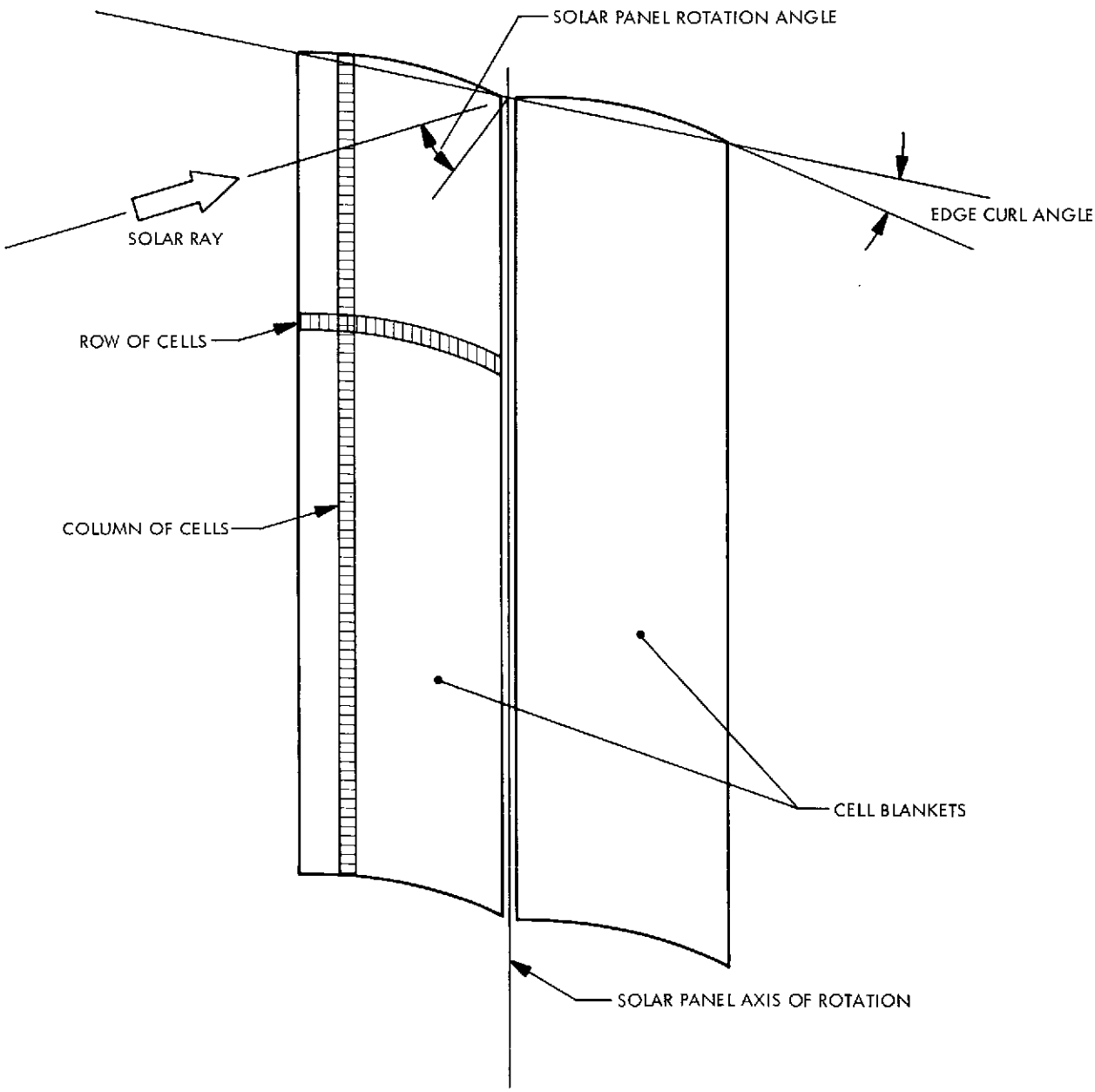

Fig. 17. Temperature Control Scheme

Figures 16 and 17 show that rotation of the solar panels can be used successfully to achieve temperature control provided the blankets can be kept fairly flat or can be made to withstand large temperature deviations. It should be kept in mind, however, that even with edge curl angles of 10 degrees, the solar panels will experience large temperature deviations only at heliocentric distances less than 0.635 AU--well past the point of Encke rendezvous.

8. Spacecraft mission trajectory. The spacecraft trajectory for 950-day Encke rendezvous mission is shown plotted in Fig. 18 and the data is tabulated in Table 14 which identifies the Heliocentric distance associated with mission time for day zero through Encke rendezvous in 20-day increments.

C. Array Configuration and Performance Prediction

To provide solar array power capability of 20 kilowatts at 1 AU, the 2.5 kW engineering model was essentially scaled up to meet the new power demand. 422,400 solar cells are required to generate the necessary power. The cells are 2 ohm-cm N on P type, 2 cm square by 0.020 cm thick, selected in accordance with the requirements and constraints identified in Section II of this document. Each cell is individually covered with 0.008 cm microsheet cover glasses. The cells are mounted on a flexible Kapton substrate and electrically assembled into 12 identical sections designed to generate equal power outputs. The solar array power requirements are summarized in Table 14. To meet the voltage range required during the mission when the solar array is normal to the sun angle, 550 solar cells are connected in series and 768 cells are connected in parallel. The combined power producing capability of the 12 electrical sections (550 series cells by 768 parallel cells) is 19,002 watts when measured at 1 AU and at a nominal temperature of 52.0°C. The power uncertainty margin is plus or minus 4.8 percent. The total blanket area required to accommodate the cells and cables is 2004 ft^2 (9.77 watts per square foot). Typical dimensions of each solar panel is shown in Fig. 19.

The solar array power output prediction of 19,002 watts at 1 AU beginning of mission includes a power margin of approximately 13.5 percent assuming the power required at one (1) AU is 16,385 watts. The 13.5 percent power contingency is assumed for cable losses, space and solar flare degradation

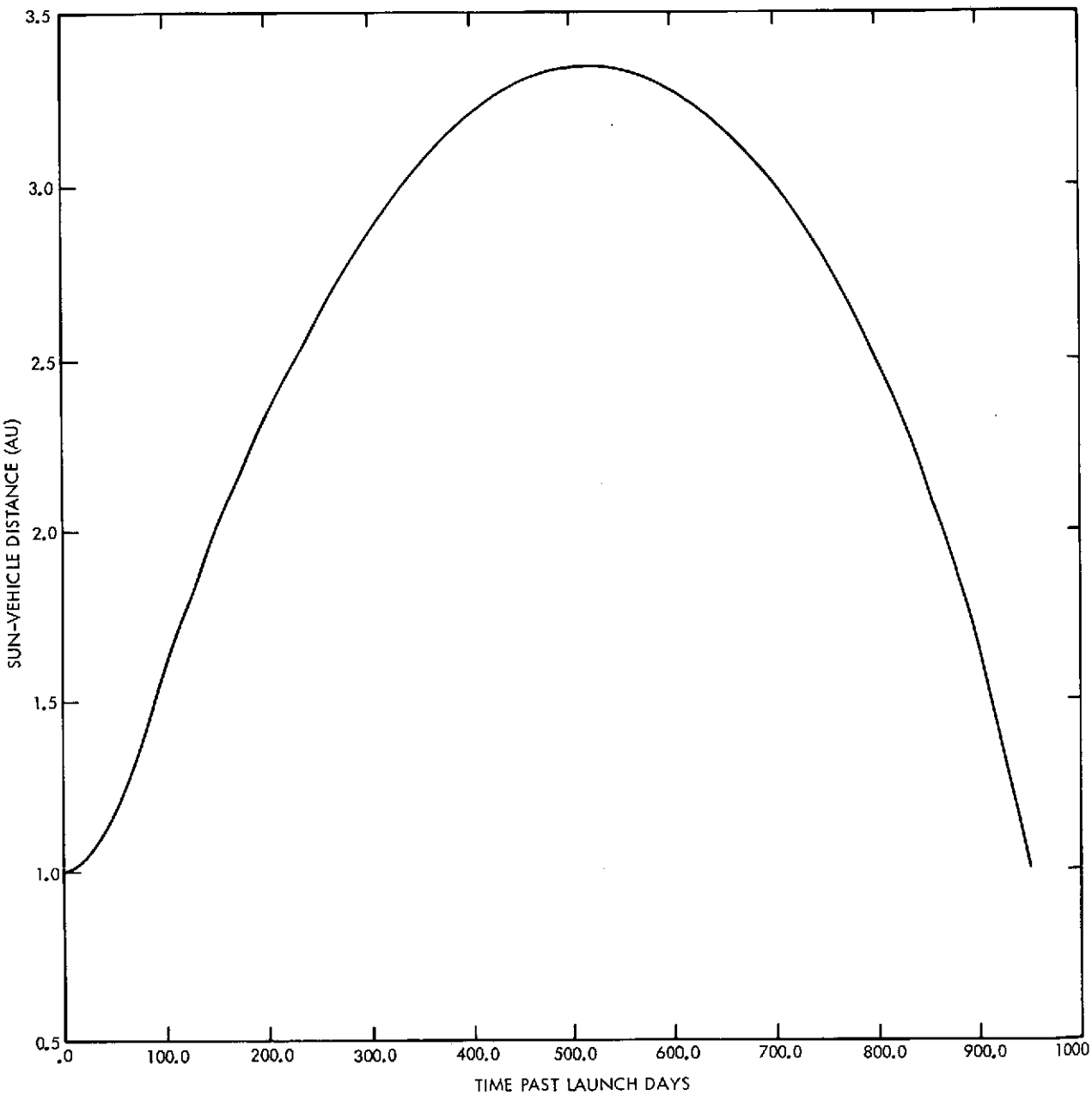

Fig. 18. Sun-Vehicle Distance

Table 14. Heliocentric Distance versus Mission Time

Time (days)	Heliocentric Distance (AU)	Time (days)	Heterocentric Distance (AU)
0	0.99472	520	3.34214
			-3.34275
20	1.01763	540	3.34148
40	1.09850	560	3.33327
60	1.22528	580	3.31740
80	1.37968	600	3.29376
100	1.54406	620	3.26217
120	1.70920	640	3.22245
140	1.86989	660	3.17434
160	2.02348	680	3.11756
180	2.16868	700	3.05175
200	2.30493	720	2.97648
220	2.43208	740	2.89123
240	2.55017	760	2.79538
260	2.65932	780	2.68816
280	2.75974	800	2.56860
300	2.85161	820	2.43549
320	2.93514	840	2.28729
340	3.01052	860	2.12195
360	3.07790	880	1.93671
380	3.13743	900	1.72773
400	3.18925	920	1.48955
420	3.23344	940	1.21432
440	3.27010	950	1.05954
460	3.29928		
480	3.32101		
500	3.33530		

which the array is expected to encounter during the mission. The predicted array power was generated utilizing the JPL M-132 computer program which includes solar array fabrication losses. Table 15 presents the power available and the degradation factors associated with power estimates at three time periods of the mission. The power profile of the array for the 950-day mission is shown in Fig. 20. Power performance degradation due to solar flare environment is based on the selection of 50 percent probability that the degradation will not be greater than 8.8 percent at the end of the 950-day mission to the comet Encke.

The solar array layout within the individual electrical sections is shown in Fig. 21, which basically configures the section into eight identical and interchangeable subsections (modules) consisting of 550 series connected submodules. The modules are designed in this manner so that they can be fabricated and tested separately and at the end of the assembly process, the modules or subsections can be mated to form a continuous blanket. The submodule design which is shown in Fig. 22 consists of eight parallel cells interconnected by a flexible expanded silver mesh.

Table 15. Solar Array Performance Prediction

Mission Time	Day 1 (1 AU)	Day 600 3.3 AU	Day 950 (1 AU)
Power available Measurement Uncertainty ±4.8% Not included	19,002 watts	2,266 watts	16,759 watts
Degradation and other losses applied	2% cable losses 1% UV deg. Total 3%	6% solar flare 2% cable losses 2% UV deg. Total 10%	8.8% solar flare degradation 2% cable losses 4% UV degradation Total 14.8%

FOLDOUT FRAME

1

FOLDOUT FRAME

2

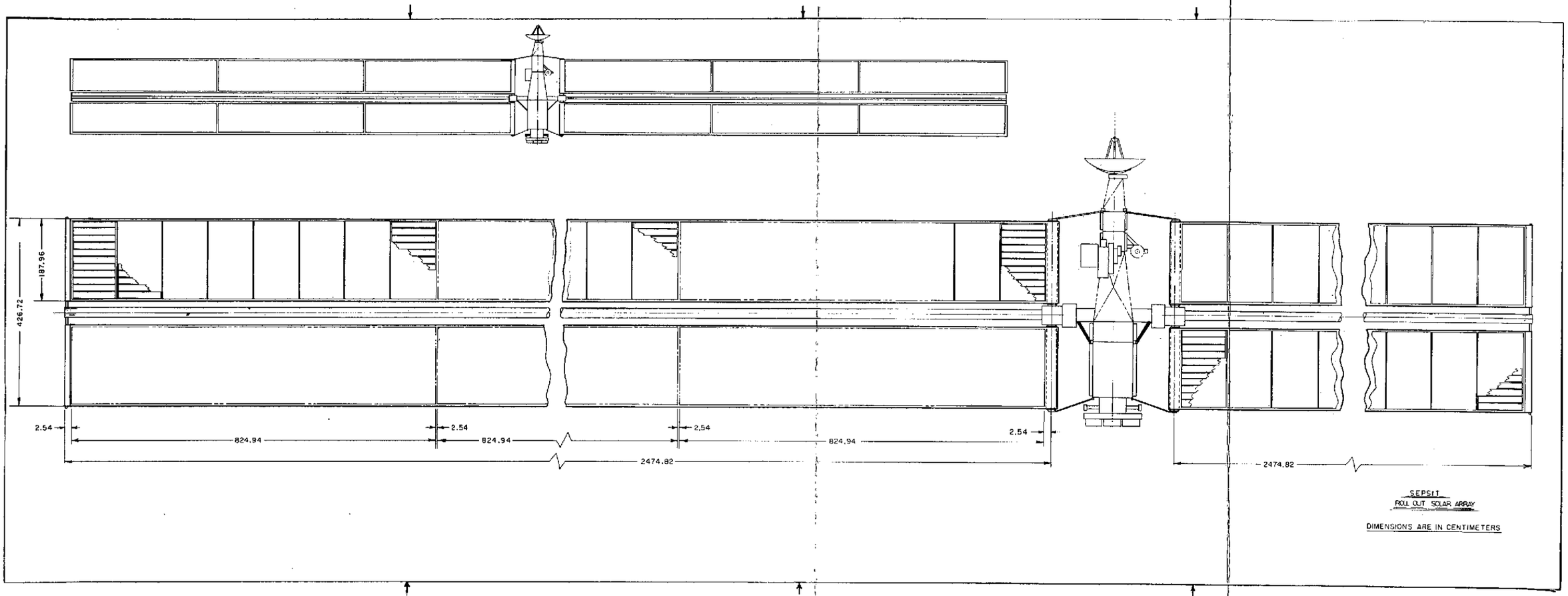

Fig. 19. SEPSIT Rollup Solar Array

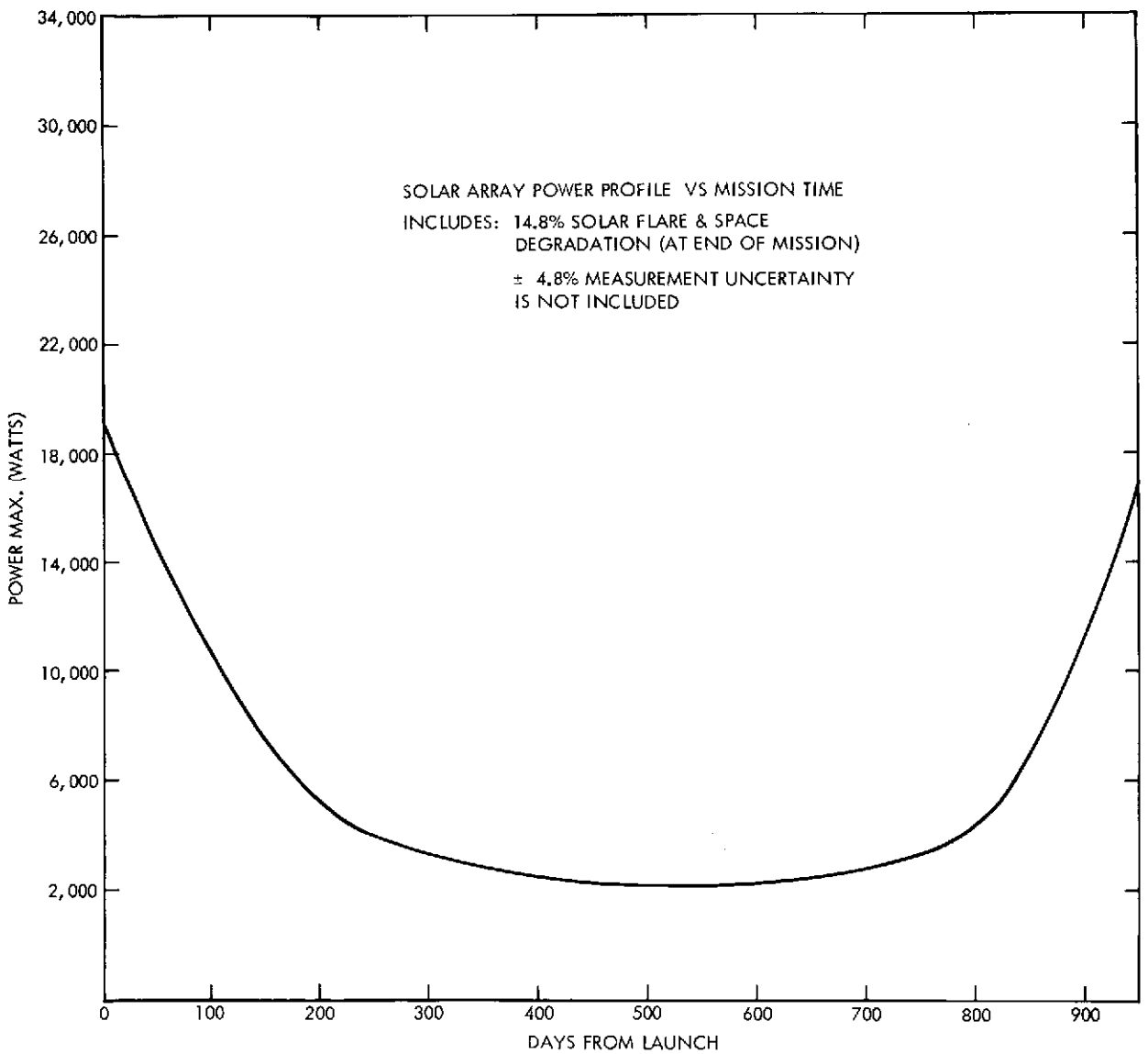

Fig. 20. Solar Array Power Profile

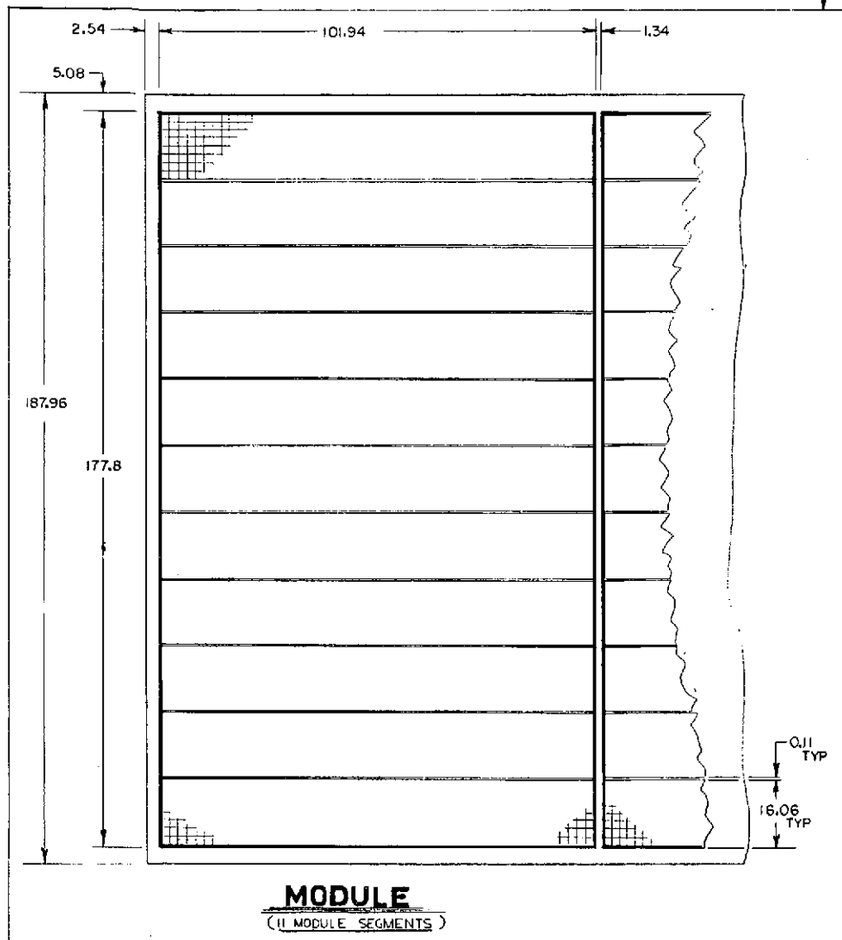

MODULE
(11 MODULE SEGMENTS)

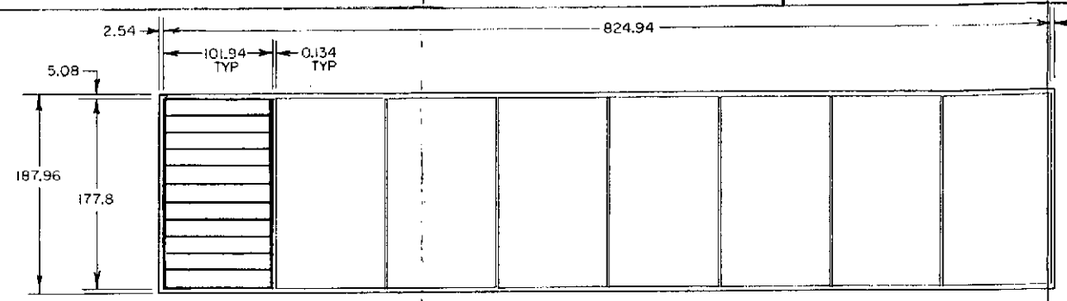

SECTION
(8 MODULES)

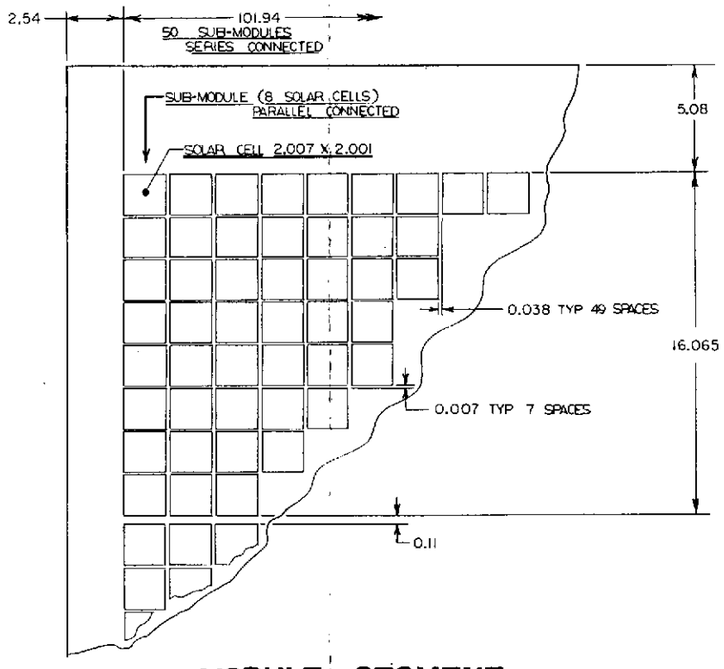

MODULE SEGMENT

8 PARALLEL CONNECTED SOLAR CELLS PER SUB-MODULE
550 SERIES CONNECTED SUB-MODULES PER MODULE
[AT 50 SUB-MODULES PER MODULE SEGMENT
AND 11 MODULE SEGMENTS PER MODULE]
8 MODULES PER SECTION
3 SECTIONS PER PANEL
4 PANELS PER ARRAY
DIMENSIONS ARE IN CENTIMETERS

Fig. 21. Module Design

PRECEDING PAGE BLANK NOT FILMED

PRECEDING PAGE BLANK NOT FILMED

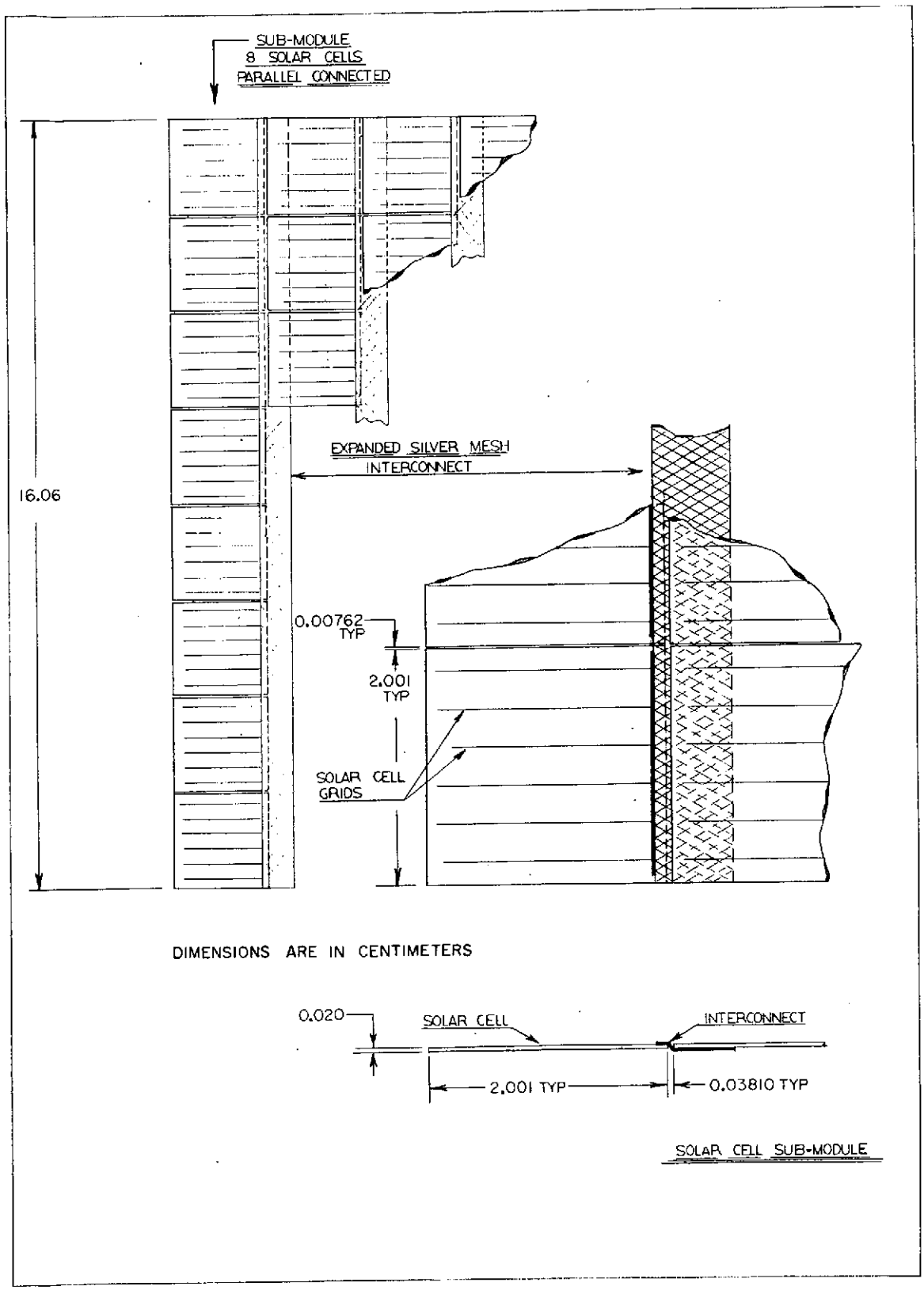

Fig. 22. Submodule Design

An independent cable from each section provides power to the slip ring assembly and to the connector interface as shown in Fig. 23. Each section cable shall be provided with a multiple conductor in flexible flat cable mechanically secured to the array substrate. Each cable section shall be sized to limit worst case power loss to two percent at rated value; provide equal voltage drop between each section and the solar array connector interface. The cable construction shall use several conductors in parallel to reduce the voltage drop, rather than one wide conductor of equivalent cross section. Detail information on cabling design and analysis is presented under Cabling Study, Section V, B, 6.

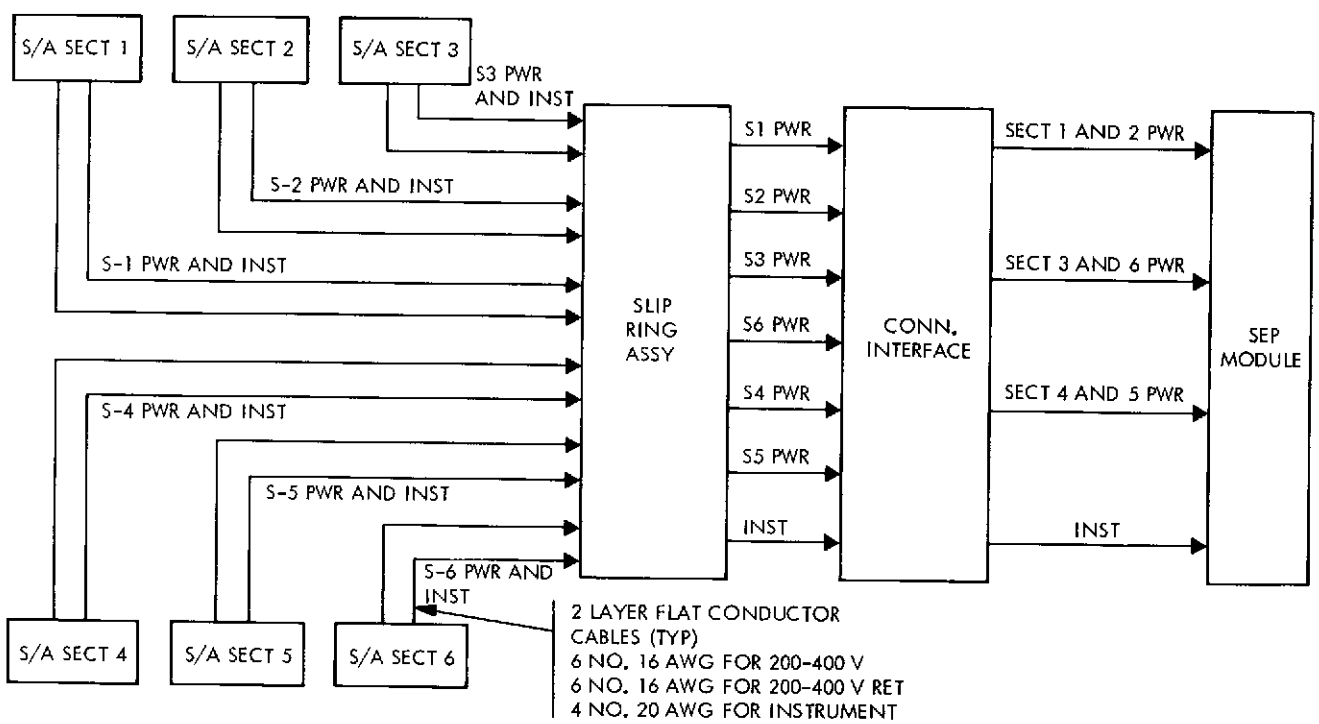

Fig. 23. Solar Array Cabling

VI. RELIABILITY CONSIDERATIONS

A survey of rigid foldout solar arrays shows that inflight failures for this type of array due to mechanical degradation have been kept to a minimum. However, the rigid foldout solar panel is of relatively simple mechanical design when compared to the rollup panels now being considered. Reliability problems associated with mechanical aspects of this new type panel will be considerably more complex and thus more emphasis must be placed on analysis and testing of the rollup panels. Electrical reliability considerations are basically the same for basic types of panels.

The mechanical considerations can be made to correspond to the following three classifications:

(1) Stowed position

(2) Deployment

(3) Deployed position

In the stowed position for launch and prior to deployment, temperature and vibration are the major degradation mechanisms to be considered. Examples of vibration effects would be fractured solar cells and open cell and/or module interconnects. In addition to vibration, compressional forces on cells may also cause cell fracture. It will be important with the present designs to allow for heat transfer from within the rolled configuration since soldered connections could be subject to degradation resulting from temperature effects.

The reliability problems for the rollup solar panels during deployment are:

(1) Pyrotechnic release failure.

(2) Panel misalignment causing

  (a) Jamming

  (b) Cell destruction on panel edge.

(3) Motor failure (functional redundancy should be considered).

(4) Adhesion and/or friction which strips off cells.

(5) Cabling - Connectors

(6) Failure of the prestressed steel to form boom tube.

In the deployed position, there are two major areas of mechanical reliability concern for the deployed solar panel. They are panel tension control and oscillation damping.

The single point failure modes for the rollup array are:

HARDWARE	FAILURE MODE
STORAGE DRUM	DRUM(s) Fail to rotate
BI-STEM Actuator	Boom fails to extend
	Premature Extension
	Boom retracts fully (in orbit)
	Length not stable (boom erected)
Solar Blanket Array	Loss of attachment to storage drum or leading edge
Outboard End Caps	Failure to release (hinge failure)
Slip Ring	High resistance (brush or ring)
NEGATOR Motor	Loss of required tension

Further analysis is required to determine the failure modes of a single cell, a module, or an electrical section and their subsequent effect on solar array power performance.

VII. AREAS REQUIRING FURTHER STUDY

A. Array Blanket Design and Fabrication

Evaluation of the array blanket design used on the GE test model indicated the need for improvements concerning fabrication, repair techniques, array flatness and modular assembly techniques. Listed below are task descriptions for introducing these improvements:

(1) Develop fabrication processes that will avoid substrate wrinkling and possibility of introducing bond voids.

(2) Develop techniques for repairing damaged cells or interconnects. Determine the permissible extent of repairs associated with factory or field incurred damage. Determine the tool, fixtures and procedures for effecting repairs for factory and field conditions.

(3) Investigate array blanket design features which will provide assurance of array flatness in the deployed state.

(4) Investigate modular assembly techniques for expediting the overall array assembly process.

B. Cell, Coverglass and Interconnect Protection

Testing of the engineering test model solar array indicated the need for improved protection for the cells, coverglass and interconnects.

(1) Cushion Design - Determine practical cushioning techniques based on the engineering test results and the effort of others in order to minimize cell and coverglass breakage. Techniques to be considered include modifications to the existing silicone rubber buttons, embossing of Kapton substrate to provide cushion zones, the use of perforated foam rubber matting bonded to the Kapton, and the application of individual padding discs.

(2) Handling Procedures - Define the procedures and handling equipment necessary to insure that damage to the array is minimized. Develop process and test flow diagrams as an aid in describing various handling conditions likely to be encountered.

C. Temperature Control Techniques and Analysis

(1) Investigate techniques for increasing the backside emissivity of rollup array blankets.

(2) Blanket stiffness as a function of temperature:

Data on the blanket bending characteristics are needed to design rewrap devices for low temperature applications.

(3) Thermal bending prediction:

Collect and analyze available data for the thermal bending of Bi-Stem deployable booms. Develop a method for predicting thermal deflection at the tip of Bi-Stem boom elements. Produce and present thermal bending predictions for Bi-Stem book elements with boom length, diameter, element thickness, material, and intensity of solar illumination as parameters.

D. Cabling Design

The GE engineering test model array utilized a copper-clad Kapton array blanket which was etched away in certain regions to form the required bus bar configuration. A significant disadvantage of this approach concerned the wrinkling of the Kapton, probably as a result of stress relief, during the etching process. The tasks required to develop an alternative approach are as follows:

(1) Investigate alternative bus bar designs considering the use of copper clad Kapton with suitable pressure sensitive adhesives. Evaluate the most practical approaches and conduct sufficient testing to determine feasibility.

(2) Establish fabrication methods and the means for electrical interconnection with solar cell strings.

(3) Determine the effects of long term space environment on cable insulation and conductors.

(4) Evaluate methods for minimizing the electromagnetic forces between conductors.

E. Slip Ring Performance Investigation

The performance data taken on the slip ring during the environmental test program of the GE test model array carried out under JPL Contract 952314 indicated noisy performance on at least two occasions. This noisy performance shall be investigated for the purpose of determining if the performance anomalies have any effect on the performance of the slip ring design in a rollup solar array on a solar electric interplanetary mission.

F. Instrumentation

Rollup solar arrays pose special constraints on flight instrumentation. The thickness of the devices is limited to permit proper wrap of the array blankets around the drums. Particular tasks aimed at developing adequate instrumentation techniques are as follows:

(1) Select thermistor devices for flight temperature measurement of solar cells on the array blanket. Develop necessary mounting, bonding and signal lead attachment techniques consistent with the thickness constraints of the solar array. Conduct sufficient testing, particularly thermal cycling, to ensure design adequacy.

(2) Establish diode requirements with particular emphasis on thickness constraints, lead attachment, environmental extremes and power rating.

(3) Investigate diode procurement with the required specifications and develop installation techniques relative to its mounting on the array blanket.

(4) Conduct environmental testing of diodes to determine adequacy of design.

G. Dynamic Loads of the Stowed Blanket

One of the principal loads to be sustained by rollup solar array structure in the stowed configuration is the dynamic loads produced by the solar array blankets. Test data accumulated on JPL/GE 66 Watts/Kg solar array (Contract 952314) show that the amplification factor at the outer wrap of the stowed solar array blanket is approximately 2 which is significantly lower than the 10 or 12

conventionally used in structural design analysis. Data on dynamic loads produced by the solar array blankets is needed to design lightweight solar array structures. The task is to provide design data in the form of blanket loads as a function of frequency in the range from 5 Hz to 100 Hz for the solar array blankets to be obtained from the engineering test model fabricated on Contract 952314. This data will be for the two cases of excitation parallel to the drum axis and perpendicular to the drum axis.

H. Environmental Tests on Solar Cells

Perform additional environmental tests on 0.020 cm thick N on P solar cells over the ranges of temperature and intensity predicted for the Encke mission.

REFERENCES

1. Gardner, J. A. "Solar Electric Propulsion System Integration Technology (SEPSIT) Final Report," Vol. III, Supporting Analyses, Technical Memorandum 33-583, Jet Propulsion Laboratory, Pasadena, California, November 15, 1972.

2. Coyner, J. V., and Ross, R. G., "Parametric Study of the Performance Characteristics and Weight Variations of Large-Area Roll-Up Solar Arrays," Technical Report 32-1502, Jet Propulsion Laboratory, Pasadena, California, December 15, 1970.

3. Ross, R. G. and Coyner, J. V., "RUSAP - A Computer Program for the Calculation of Rollup Solar Array Performance Characteristics, Users Manual, Technical Memorandum #33-634, Jet Propulsion Laboratory, Pasadena, California, In Publication.

4. Solar Electric Multimission Spacecraft (SEMMS) Phase A Final Report, Spacecraft Subsystem Analyses, Doc. 617-4, Jet Propulsion Laboratory, Pasadena, California, March 17, 1972 (JPL internal document).

5. J. R. Carter Jr and H. Y. Tada, "Solar Cell Radiation Handbook" TRW Systems Group, Redondo Beach, California, June 28, 1973.

6. Arnett, J., and Bunker, E. R., Jr., "SEP Solar Panel Cable Interconnection Study" (JPL internal document 357-RHD-73-41).

7. Anspaugh, B. E. "Uncertainties in Predicting Solar Panel Power Output" (JPL internal document).

NASA — JPL — Coml., L.A., Calif.